

## Molecular Modeling: A Search for a Calpain Inhibitor as a New Treatment for Cataractogenesis

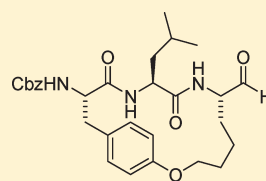
Blair G Stuart,<sup>†</sup> James M. Coxon,<sup>\*,†</sup> James D. Morton,<sup>\*,‡</sup> Andrew D. Abell,<sup>†,||</sup> D. Quentin McDonald,<sup>§</sup> Steven G. Aitken,<sup>†</sup> Matthew A. Jones,<sup>†</sup> and Roy Bickerstaffe<sup>‡</sup>

<sup>†</sup>Univesity of Canterbury, Christchurch, New Zealand

<sup>‡</sup>Lincoln University, Lincoln New Zealand

<sup>§</sup>Q-Bit Ltd., Christchurch, New Zealand

**ABSTRACT:** Studies of 17 analogs of 3 (SJA6017) in an in silico calpain model are reconciled to measured IC<sub>50</sub> values against ovine calpain. The studies validate the potential of the “model” and criteria established for inhibition as a tool to select structures for synthesis to test as calpain inhibitors. Using this screening methodology of virtual libraries led us to synthesize several inhibitors including macrocycle 33, which in vitro sheep eye lens culture experiments showed to substantially slow opacification.



slows opacification  
in sheep eye lens  
culture experiments

### INTRODUCTION

There is evidence in animal models that the cysteine protease, calpain, is involved in cortical cataract.<sup>1–4</sup> Our studies are directed to reducing the rate of cataractogenesis by inhibiting lens calpains, and herein we use in silico models of calpain isoforms to facilitate the selection of calpain inhibitor templates and structures that could have the potential to reduce the rate of cataractogenesis.

Knowledge of the active site of calpain is crucial for our modeling studies, and the coordinates established from X-ray studies are essential.<sup>5</sup> There is evidence that some forms of cataract are a metabolic outcome of unregulated Ca<sup>2+</sup> mediated degradation of lens crystallins.<sup>6–15</sup> Crystallins are highly soluble proteins located in eye lens that form a clear array due to the specific protein–protein packing.<sup>8–15</sup> Any degradation of the crystallins can disrupt their packing, and as a consequence, precipitation occurs which is known as cataractogenesis.<sup>8–15</sup> One isoform of calpain,<sup>16,17</sup> *m*-calpain (calpain 2, CAPN2), is predominant in lens and is the major enzyme considered responsible for cataracts in rodent models. An increase in the activity of this enzyme is initiated by any increase in Ca<sup>2+</sup> levels resulting from damage of the eye through long-term exposure to ultraviolet light or other injuries. Inhibition of CAPN2<sup>18</sup> would therefore be expected to retard cataract formation, and consequently, calpain inhibitors are potential therapeutic drugs for slowing cataractogenesis.

The two best characterized calpain isoforms, calpain 1 (CAPN1) and CAPN2,<sup>19,20</sup> are both heterodimers with six domains and exhibit high structural homology, each composed of two subunits. The large 80 kDa catalytic subunit is made up of domains I–IV and the smaller 30 kDa regulatory subunit of domains V and VI. Binding of calcium at DIV and DVI causes the catalytic triad in the active site at DII to adopt the active proteolytic conformation. The first reported calpain crystal structures<sup>21,22</sup> showed the active site of the enzyme to be in a

nonactive conformation. There are difficulties associated with cocrystallizing calpain in the presence of Ca<sup>2+</sup> and thereby in an active conformation because calpain in the presence of calcium is autoproteolytic and self-hydrolyzes into fragments, destroying its activity.<sup>23–26</sup> Several plant cysteine proteases however, including papain, have been reported with the catalytic triad in the active conformation. It is the coordinates of the catalytic site in the active conformation that are important for our modeling studies. The proposed mechanism of action of a cysteine protease is that concomitant with substrate binding there is deprotonation of the active site cysteine thiol and protonation of the histidine.<sup>27–29</sup>

A construct made up of domains IIa and IIb of each of CAPN2 and CAPN1 provide coordinates from which a model can be developed for testing potential inhibitors, as these two mutated calpain constructs<sup>30</sup> both display the catalytic triad in an active conformation.<sup>25,26</sup> The protease core of the CAPN1 construct (PDB code 1KXR) has been crystallized in the presence of Ca<sup>2+</sup> in which the active site Cys115 was mutated to Ser115 preventing autolysis. The active site of 1KXR (Figure 1) superimposed on the active site of papain (PDB code 1PPN) shows the close superimposition of critical active site residues including the catalytic triad of Cys115 (papain Cys25), His272 (papain His159), and Asn296 (papain Asn175). The nonmutated construct, analogous to 1KXR, is generated during autolysis of native CAPN1 enzyme and is a stable fragment that is inactive in the absence of Ca<sup>2+</sup> but active in the presence of Ca<sup>2+</sup>.

The mutated protease construct core of CAPN2 (PDB code 1MDW)<sup>26</sup> in the presence of Ca<sup>2+</sup> has also been crystallized, but unlike the CAPN1 construct it is not active in the presence of Ca<sup>2+</sup> in vitro. The crystal structure data showed that residues 198–201 (Figure 2) within the  $\alpha$ -helical region ( $\alpha 7$ ) displayed no electron density, and it is thought<sup>26</sup> that flexibility of this

Received: May 30, 2011

Published: September 28, 2011

glycine rich region (residues 197, 198, and 203) results in the side chain of Trp106 blocking the active site pocket (Figure 3), providing a rationale for autoinhibition.

There are a number of natural calpain inhibitors<sup>31,32</sup> including the endogenous inhibitor calpastatin composed of four repeating domains that contribute to the inhibitory qualities and an N-terminal domain (domain L) that by itself displays no inhibition.<sup>33</sup> There are also some derived from microbes, includ-

ing *Streptomyces* fungi of which leupeptin, antipain, and strepin P-1 are examples<sup>34</sup> of inhibitors that react reversibly with the enzyme's active site thiol.<sup>35</sup>

The X-ray crystal structure of leupeptin in complex with CAPN1 construct (1TL9)<sup>36</sup> (Figure 4) shows (left diagram) that the inhibitor is covalently bound between the carbon of the aldehyde warhead and the sulfur of Cys115 and that three hydrogen bonds are present between the leupeptin backbone and Gly271 and Gly208 of the enzyme. These three hydrogen bonds have been found in a number of inhibitor–calpain complexes, including the E64–CAPN1 construct (1TL0),<sup>36</sup> SNJ-1715–CAPN1 construct (2G8E),<sup>37</sup> and ZLAK-3001–CAPN1 construct (2R9C),<sup>38</sup> and the presence of these hydrogen bonds is considered of intrinsic importance for potent inhibition.

Of the two constructs 1KXR and 1MDW the former was chosen for our modeling studies because the unmutated version of the construct displayed activity in vitro whereas the unmutated construct of 1MDW did not.

The known calpain inhibitor 3 (SJA6017)<sup>40</sup> has been identified by us as a suitable initial lead compound for our modeling studies. This compound, as with many inhibitors including leupeptin, antipain, and strepin P-1, contains three regions (Figure 5): a warhead, a central region usually consisting of two or three amino acids that we now know must exhibit a propensity for a  $\beta$ -strand conformation, and P2-Cap region at the end opposite the warhead. An aldehyde “warhead” can undergo oxidation under cellular conditions, so there is interest in finding alternative electrophilic warheads.<sup>34</sup> IC<sub>50</sub> data for 3 and 17 analogues determined using rat CAPN1 and a BODIPY fluorescent microplate assay have been reported.<sup>40</sup> As these compounds have a common framework but

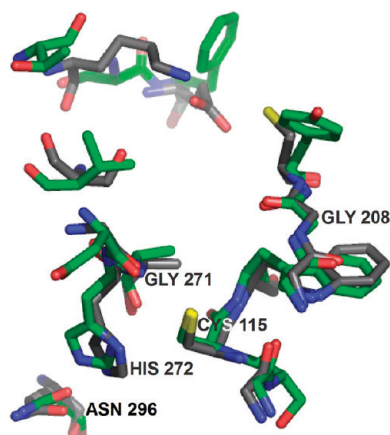


**Figure 1.** Active site of CAPN1 construct (1KXR) with gray carbons superimposed on active site of papain (1PPN) with green carbons. Residues named are for 1KXR, including the catalytic triad of Cys115 (mutated in silico from Ser115), His272, and Asn296. The equivalent papain residues are Cys25, His272, His159, and Asn175, respectively.



**Figure 2.** Part sequence of 1MDW (residues 175–236) and the equivalent part sequence of 1KXR (residues 185–246). The red tubes indicate regions of  $\alpha$ -helices. Blue arrows indicate regions of  $\beta$ -sheets. The red residue letter codes indicate nonconserved residues between CAPN1 and CAPN2.<sup>25,26</sup>

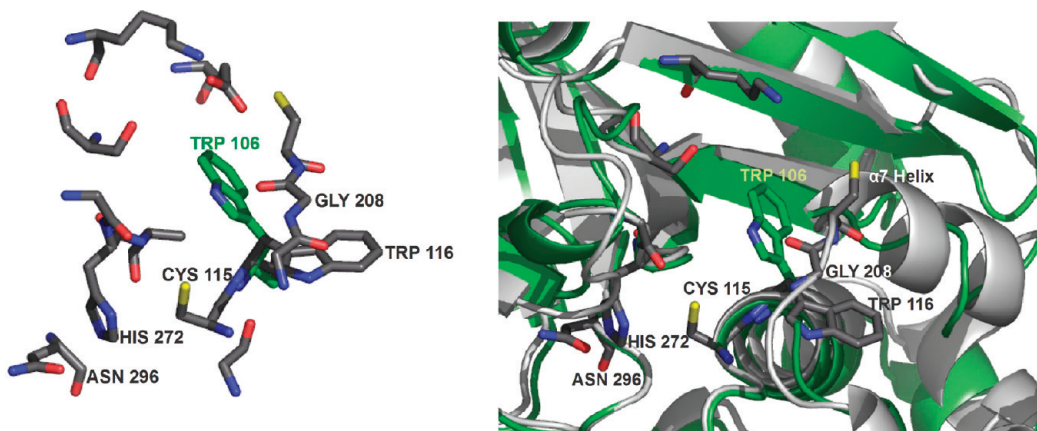


**Figure 3.** Left: Active site of 1KXR (gray) superimposed on active site of 1MDW (green) showing Trp116 of 1KXR in the active conformation and the equivalent Trp106 of 1MDW blocking the active site. Right: Active site of 1KXR (gray) superimposed on active site of 1MDW (green) showing the  $\alpha$ 7 helix of 1KXR intact and the equivalent region of 1MDW in a disordered state with missing residues due to no observable electron density.

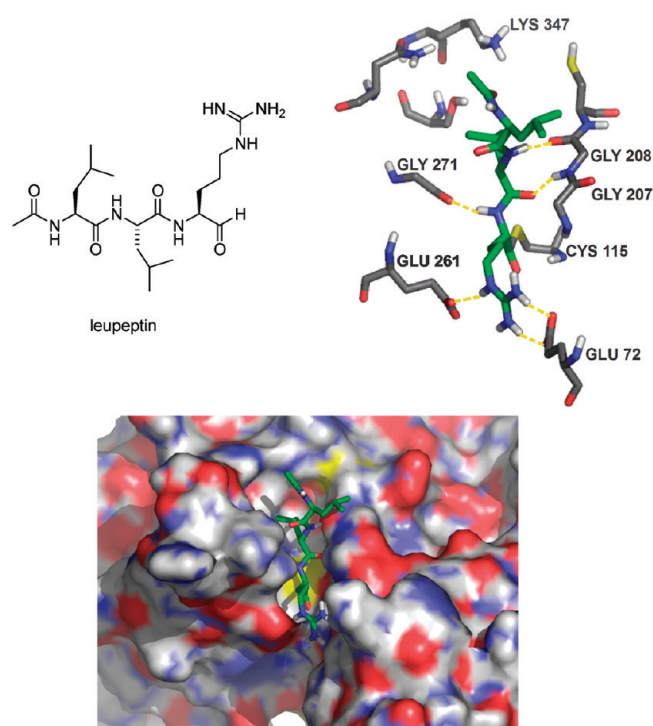


**Figure 4.** Leupeptin and X-ray structure of leupeptin in complex with CAPN1 construct (1TL9). Above right: Enzyme depicted as sticks, leupeptin as tubes. Below: Surface model of enzyme with leupeptin as tubes stretched along the cleft of the enzyme.<sup>39</sup>

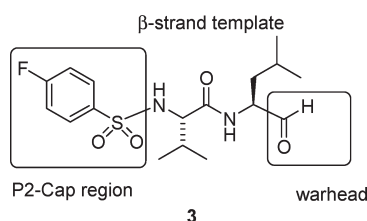


**Figure 5.** The three regions of 3.

exhibit subtle changes that produce considerable variations in  $IC_{50}$  values, the series is therefore ideal to assess the modeling methodology.

## RESULTS AND DISCUSSION

We now report on the utilization of the coordinates of the mutated CAPN1 construct, 1KXR, to model and examine a series of analogues of **3** that are calpain inhibitors of known activity. This approach was undertaken to establish whether current modeling methodology can provide an understanding of the differences in inhibitory activity of known inhibitors and thereby establish whether the modeling approach would be a useful predictive tool for identifying structures and their characteristics that would predispose them to be inhibitors. This is followed by modeling studies of a series of heterocyclic structures and macrocyclic analogues of **3** where the potential of such compounds as inhibitors was initially unknown. The results of these studies led to us preparing a number of compounds and in vitro testing of the more promising compounds.

**The Enzyme Model and Its Validation.** We have evaluated by docking studies the series of analogues of **3** (Table 1) to test our

calpain “model” and to determine if we could rationalize the reported  $IC_{50}$  data. The development of the model was predicated by our interest in being able to evaluate potential inhibitors, thereby defining candidates for synthesis. For our studies the crystal structure 1KXR was first mutated in silico with the Ser115 replaced by Cys115 to produce a model that approximates that of an active construct.<sup>41,42</sup> The oxygen of the serine was replaced by sulfur, and the bond lengths and angles were corrected by minimization. The active site of the “model” is a narrow cleft bordered by two steep sides that are made up of domain I (Figure 6 left, left-side) and domain II (Figure 6 left, right-side). The two ends of the cleft, with Cys115 as the center, are known as the C-terminus prime side and the N-terminus nonprime side.<sup>43</sup> Deep within this nonprime region are regions of hydrophobicity (Figure 6 center) depicted as copper colored and suitable to accommodate hydrophobic amino acid side chains of any bound ligand. Areas of hydrophilicity (Figure 6 right), shown in pale blue, surround the active site and can accommodate hydrophilic groups of a bound inhibitor.

In order to facilitate the docking studies of the analogues of **3** into this above model, each analogue was first subjected to a Monte Carlo conformational search and the lowest energy conformer that displayed a  $\beta$ -strand conformation was used as an input structure for docking into the active site of the calpain “model.”<sup>44</sup> Fairlie<sup>45,46</sup> has previously reported the importance of a  $\beta$ -strand for bioactivity. The docking parameters for the best pose of a possible 10 poses generated and collected by Glide and the inhibitory concentrations ( $IC_{50}$ ) for the compounds are shown in Table 1. In the examination of poses, consideration is given to the relative position of the cysteine sulfur and the  $\pi^*$ -orbital of the carbonyl, recognizing the Dunitz trajectory for nucleophilic attack. Only poses where the carbonyl carbon is within 4.5 Å of the sulfur were considered, this distance being regarded as an outer limit for flexibility of and in the active site to allow nucleophilic attack by the sulfur of cysteine and reversible thioacetal formation.

GlideScore is a scoring function designed to estimate free energy of binding for a protein–ligand complex. The function uses simple contact terms to estimate lipophilic and metal–ligand binding contributions, a simple explicit form for hydrogen bonds and a term that penalizes flexibility. The Emodel is a model energy score that combines energy grid score, binding affinity predicted by GlideScore, and for flexible docking the internal strain energy.<sup>71,72</sup>

The amino acid residues that surround the N-terminal nonprime side of the inhibitors in the active site are shown in Figure 7 along with Cys115, the active site nucleophilic residue that facilitates cleavage of peptide substrates. On either side of Cys115 are the residues Gly208 and Gly271, respectively, which the modeling studies show to be important in forming H-bonds to peptide based ligands in a  $\beta$ -strand conformation.<sup>47</sup>

In each case the “best pose” is chosen by four criteria in the following order of importance: (i) presence of the three essential hydrogen bonds that stabilize a  $\beta$ -strand conformation of an inhibitor, (ii) a warhead distance of less than 4.5 Å between the warhead electrophilic carbon and the nucleophilic sulfur of Cys115, (iii) a low Glide score/Emodel score, and (iv) the lowest number of internal ugly contacts where there is a contact distance of <75% of the sum of the van der Waals radii.

Compounds **1** and **2** are potent inhibitors of CAPN1 and have low negative Glide and Emodel scores and exhibit the three hydrogen bonds considered essential for appropriate binding in

Table 1. Docking Data for Best Pose for 1–18<sup>a</sup>

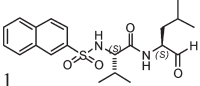
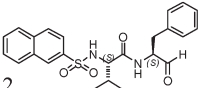
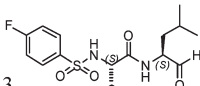
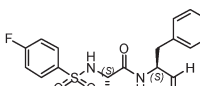
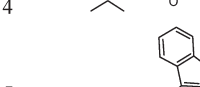
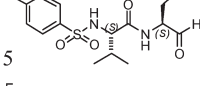
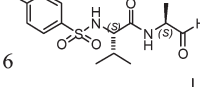
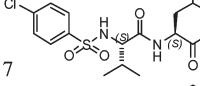
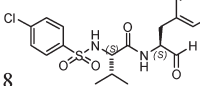
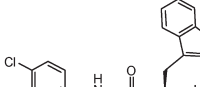
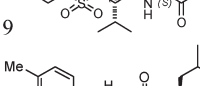
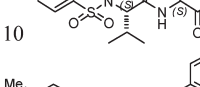
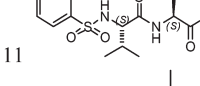
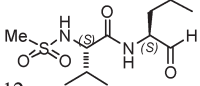
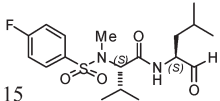
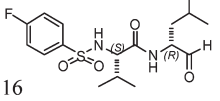
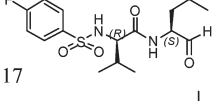
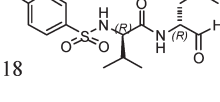
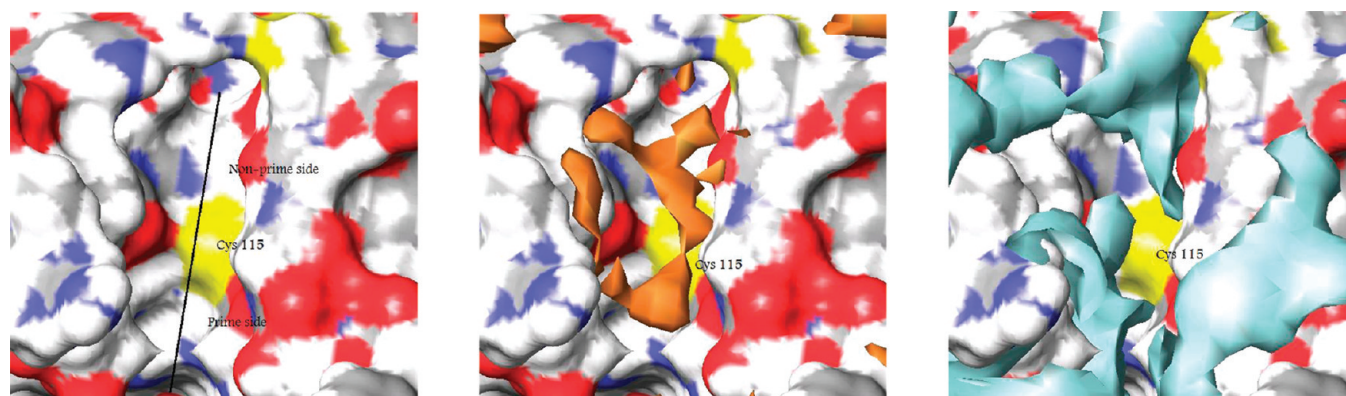
Structure	Glide Score	Emodel Score	Essential H bonds	Warhead Distance Å	Internal contacts			IC <sub>50</sub> (nM) CAPN1
					Good	Bad	Ugly	
 1	-4.6	-52.1	3	3.9	200	9	0	10
 2	-5.4	-60.6	3	3.7	197	14	0	14
 3	-5.8	-49.4	3	4.2	203	9	0	7.5
 4	-5.9	-54.7	3	4.0	205	14	0	27
 5	-4.6	-59.3	3	3.6	195	7	0	23
 6	-4.8	-49.9	3	4.1	139	10	1	630
 7	-4.5	-45.9	3	4.0	189	11	1	31
 8	-4.9	-55.5	3	3.7	175	10	0	14
 9	-6.1	-62.4	3	3.4	212	10	0	13
 10	-5.6	-50.7	3	3.9	216	18	1	28
 11	-6.0	-54.7	3	4.9	205	9	0	18
 12	-5.9	-48.2	3	3.7	188	9	2	830
 13	-4.6	-49.2	2	4.0	188	20	3	130
 14	-4.0	-52.7	2	3.6	212	15	0	260



Table 1. Continued

Structure	Glide Score	Emodel Score	Essential H bonds	Warhead Distance Å	Internal contacts			IC <sub>50</sub> (nM) CAPN1
					Good	Bad	Ugly	
 15	-2.4	-45.9	1	4.4	217	15	0	21000
 16	-4.6	-52.0	3	>5	191	15	1	14000
 17	-3.4	-50.9	3	4.3	233	21	10	42000
 18	-4.6	-46.3	2	3.8	206	13	5	1000000

<sup>a</sup> Inhibitory concentrations (IC<sub>50</sub>) as reported by Inoue et al.<sup>40</sup>



**Figure 6.** Left: Surface diagram of 1KXR showing the active site cleft (black line) with the active site Cys 115 in yellow. Above the Cys 115 is the nonprime side, and below is the prime side. The active site is a deep valley with high sides. Center: Copper areas depict regions of space on the surface of the enzyme that are hydrophobic. Deep within the nonprime side are areas of hydrophobicity. Right: Pale blue areas depict regions of space on the surface of the enzyme that are hydrophilic. Some surrounding areas just out of the pocket are hydrophilic. The surface is defined using the site map tool in Maestro.

the active site. The distance between the warhead and nucleophilic cysteine sulfur is less than 5 Å, allowing for nucleophilic attack. They also have no bad internal contacts, termed “ugly” contacts. The X-ray crystal structures (1TL9 and 1TL0) of truncated calpain enzymes cocrystallized with two well-known calpain inhibitors,<sup>36</sup> together with X-ray crystal structures of other proteases, support the hypothesis that there are three key H-bonds that result in and from a  $\beta$ -strand conformation of the inhibitor binding to two glycine residues in the active site. Specifically Gly208 and Gly271 are important for stabilization of the bound ligand in a  $\beta$ -strand conformation, and bound in this way the ligand’s warhead is in a position for nucleophilic attack by the active site cysteine (Cys115)<sup>27,45,46,48,56,57</sup> (Figure 8).

The “best poses” of **1** and **2** (Figure 9) with their backbones depicted as tubes exhibit the ligand in a  $\beta$ -strand conformation and oriented to form the three essential hydrogen bonds, one with Gly271 and two with Gly208. The naphthalene capping

group of each is pointing out of the pocket and sitting over the Gly208 and Cys209 residues. This is similar to how the inhibitor leupeptin binds to the CAPN1 construct as is seen in the X-ray structure 1TL9.<sup>36,39</sup> This is shown in Figure 10 by a stereodialog of a docked pose of **3** in 1KXR overlaid with crystal structure of leupeptin covalently bound in the active site. Modeling shows that **3** along with similar molecules arrange in the same orientation, with the same three critical H-bonds and in a  $\beta$ -strand conformation as exhibited by leupeptin covalently bound in calpain.

Compounds **3–6** (Figure 9 right) dock in a manner similar to **1** and **2** but with different orientations of their 4-fluorophenylsulfonyl groups. The capping groups of **3** and **4** point back over the  $\beta$ -strand backbone of the molecule, and in **5** and **6** the capping groups are directed toward Lys 347. Compounds **3**, **4**, and **5** are potent inhibitors, and the docking data show that they have low negative Glide scores and Emodel scores and exhibit the

three essential hydrogen bonds and have a distance between the warhead and nucleophilic cysteine sulfur less than 5 Å. Compound **6** has a higher  $IC_{50}$  than **1–5**. The main difference

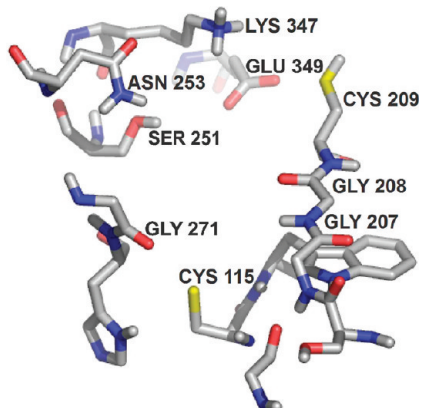


**Figure 7.** Active site of the calpain Glide model based on the PDB structure 1KXR showing the residues surrounding the nonprime region.

between **6** and **1–5** is the size of the side chain at the  $P_1$  position: **6** has an alanine at the  $P_1$  position, and the methyl side chain has less potential for lipophilic interactions than the other compounds with larger nonpolar side chains at the  $P_1$  position. Compound **6** had the highest (less favorable) lipophilic interaction energy calculated for all compounds in the series. The  $P_1$  side chains are close to Leu260 and positioned to form lipophilic interaction with the nonpolar side chain of Leu260. The larger  $P_1$  side chains of **1–5** allow for less movement within the active site. The best fit pose of compound **6** also has one “ugly” internal contact.<sup>49</sup>

We have measured<sup>50</sup> the inhibition characteristics of **3** that we independently synthesized and evaluated against o-CAPN2 and o-CAPN1. The  $IC_{50}$  values were 80 and 130 nM, respectively, and these values are compared with a value of 7.5 nM reported by Inoue<sup>40</sup> as measured against rat CAPN1.

Compounds **7**, **8**, and **9** are good inhibitors of CAPN1 and exhibit similar docking data as the potent inhibitors identified above. The differences are at the  $P_1$  position. Compound **7** has a slightly higher  $IC_{50}$  to **8** and **9** and has an “ugly” internal contact in the best pose.

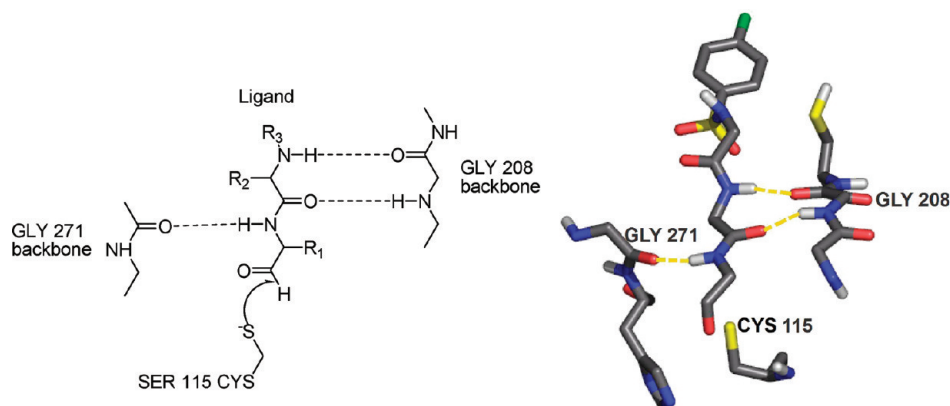


**Figure 8.** Left: Schematic diagram of a typical peptidomimetic ligand docked in the active site of mini CAPN1 according to the X-ray structure (1KXR) before attack from CYS115. The formation of  $\beta$ -sheet type H-bonding between the ligand and the backbone of two GLY residues is a requirement of good binding and therefore good inhibition. In addition, the electrophilic warhead needs to be in a position for nucleophilic attack by the S of CYS115, typically within 5 Å. Right: Picture of a typical peptidomimetic ligand docked into our model active site derived from the X-ray structure of mini CAPN1 (1KXR). The amino acid side chains of the ligand have been omitted for clarity.

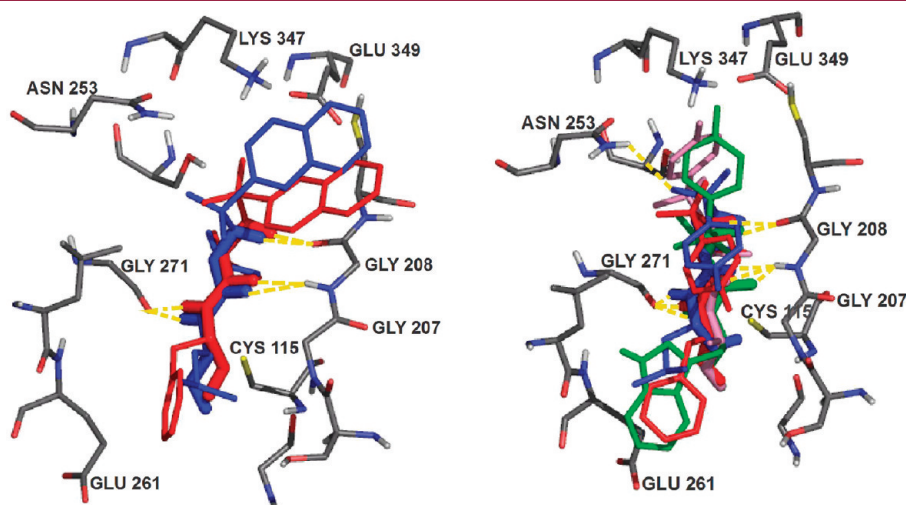


**Figure 9.** Left: Best docked poses of compounds **1** (blue) and **2** (red). Right: Best docked poses of compounds **3** (blue), **4** (red), **5** (green), and **6** (pink).

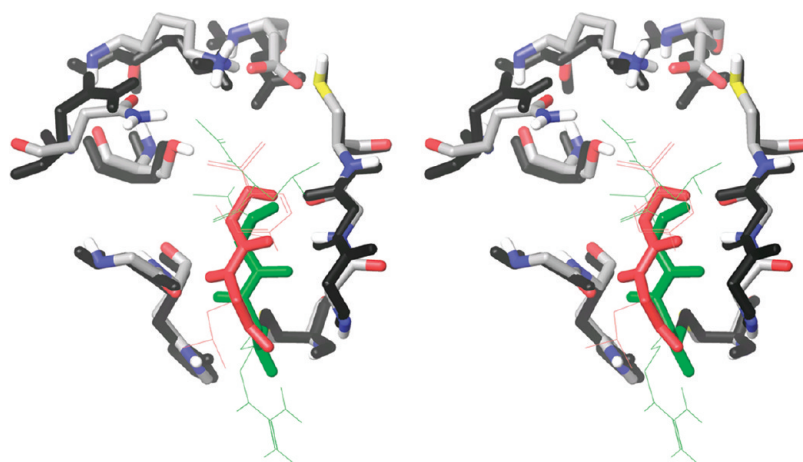


**Figure 10.** Stereodiam of the best docked pose of **3** (red) docked into 1KXR (gray carbons) overlaid with crystal structure of 1TL9 (black), which has leupeptin (green) bound covalently in the active site.

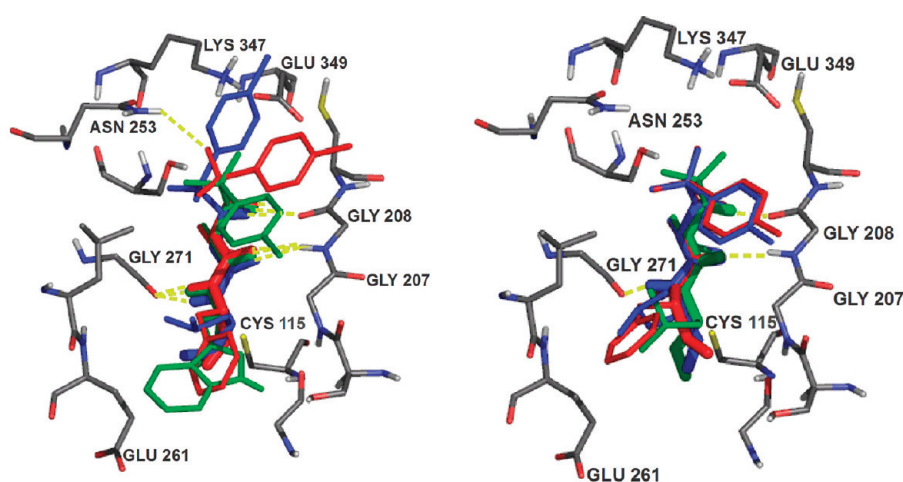


**Figure 11.** Left: Best docked poses of compounds **7** (blue), **8** (red), and **9** (green). Right: Best docked poses of compounds **10** (blue), **11** (red), and **12** (green).

The best poses for **10**, **11**, and **12** (Figure 11) have low negative Glide scores and Emodel scores, the three essential hydrogen bonds, and appropriate warhead–nucleophile distances. Compound **11** has the lowest  $IC_{50}$  of these three compounds, and the docking study shows no repulsive interactions. Compound **10** with a slightly higher  $IC_{50}$  has one “ugly” internal contact, and **12** has an  $IC_{50}$  of >100-fold higher than **3** with two “ugly” internal contacts. It has a methylsulfonamide capping group compared with the larger capping group (e.g., 4-fluorophenylsulfonamide) of the other compounds and is less able to form favorable hydrophobic interactions with the enzyme pocket than the larger capping groups which also have a halogen that can form H-bonds.

Compounds **13** and **14** have a L-Nval or L-Nle at  $P_2$ , respectively, compared to **1** and **12** with L-Val at this position. When **13** and **14** dock into the active site with the  $P_2$  position fitting into the deep hydrophobic pocket ( $S_2$ ) in the active site cleft, L-Val has a good fit in this pocket while L-Nval and L-Nle do not fit the pocket well and alter the position of the  $\beta$ -strand backbone in relation to the hydrogen bond forming Gly271 and Gly208 residues. Consequently both **13** and **14** have only two of

the three hydrogen bonds considered essential and **13** has three “ugly” internal contacts accounting for the higher  $IC_{50}$  values of only 130 and 260 nM, respectively. Compound **15** is structurally similar to the most potent compound **3** but with a methyl group replacing a hydrogen atom (Table 1). When **3** and most of the other compounds are docked, this hydrogen position forms one of the hydrogen bonds considered essential to the backbone oxygen of Gly208. The substitution of the hydrogen for a methyl group in **15** removes the potential of the ligand to form this hydrogen bond. The methyl group is also bulkier and forces the ligand to twist in order to fit into the pocket (Figure 12). Only one of the three essential hydrogen bonds is formed and the compound has a poor Glide score of  $-2.4$  and a poor  $IC_{50}$  of 21 000 nM.

Compounds **16**, **17**, and **18** differ from **3** in that one or both amino acids have a D-configuration instead of the normal L and all have poor  $IC_{50}$  values. The difference in chirality has a detrimental effect for ligand binding. Compound **16** has a D-Leu at the  $P_1$  position, and with the three essential hydrogen bonds present the aldehyde warhead is not positioned close to the nucleophilic cysteine sulfur. Compound **17** has valine at the  $P_2$  position in a



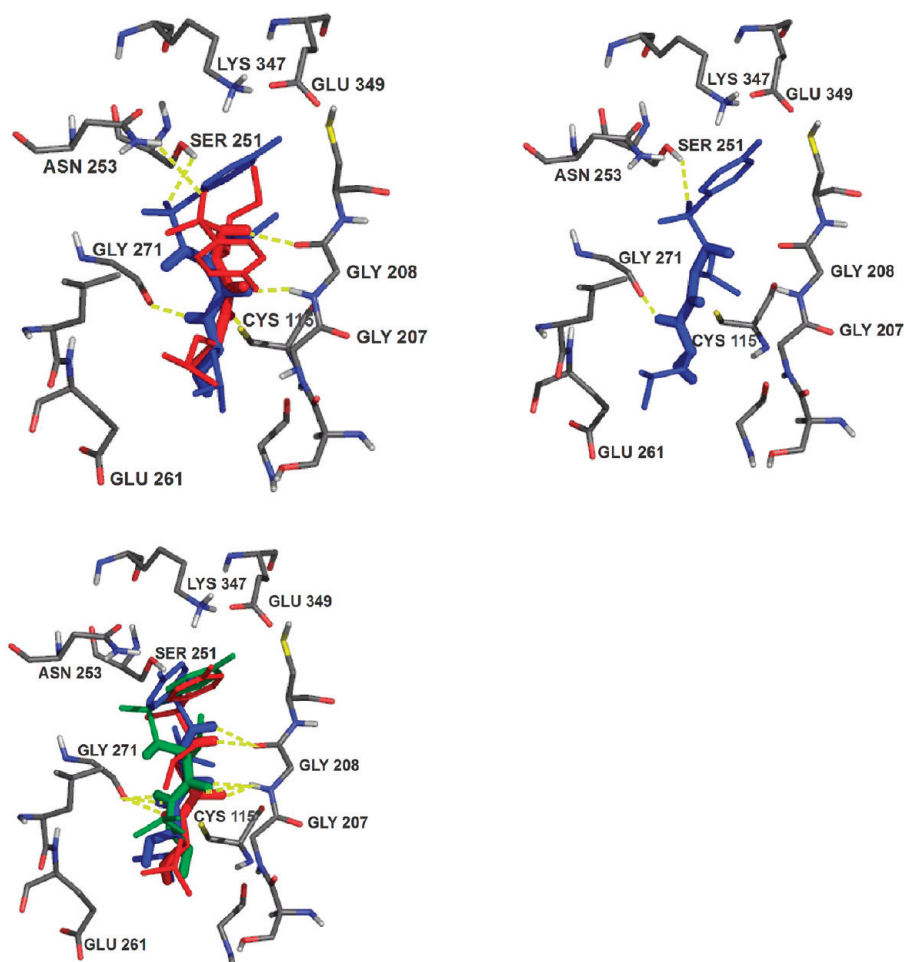


**Figure 12.** Upper left: Best docked poses of compounds 13 (blue) and 14 (red). Upper right: Best docked pose of compound 15 (blue). Lower left: Best docked poses of compounds 16 (blue), 17 (red), and 18 (green).

D-configuration and a pose with the three appropriate hydrogen bonds and with a close warhead–cysteine distance has 10 “ugly” internal contacts.<sup>51</sup> The docked pose of 17 (Figure 12) shows that the side chain of the D-Val is pointing out of the active site pocket instead of deep in the hydrophobic region of the cleft where the P<sub>2</sub> side chain is found in poses of the more potent dipeptide ligands. The loss of this seemingly crucial hydrophobic contact is reflected by the poorer Glide score of −3.4. Compound 18 has both the P<sub>1</sub> and P<sub>2</sub> amino acids in a D configuration, and the best docked pose shows that it can only form two of the three required hydrogen bonds when the warhead is in a position for nucleophilic attack. In order to achieve this pose, five “ugly” internal contacts form, most of which involve the proximity of the P<sub>2</sub> side chain and the capping group end which is an unfavorable conformation.

Of the 18 compounds studied, 1–5, 8, 9, and 11 have IC<sub>50</sub> values of less than 30 nM against CAPN1. The best poses for these compounds show a warhead–cysteine sulfur distance of less than 5 Å, an appropriate distance necessary for nucleophilic attack to occur on the aldehyde and in a position for reversible covalent bond formation. They meet the requirement of having the three essential hydrogen bonds, an important constraint of a β-strand moiety. Their P<sub>1</sub> side chains form hydrophobic contacts with Leu260, and their P<sub>2</sub> side chains fit deep into the hydrophobic pocket of the active site. The poses show no “ugly”

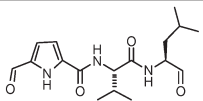
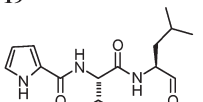
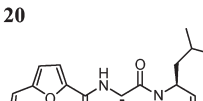
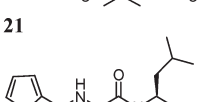
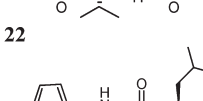
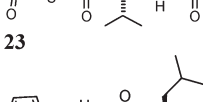
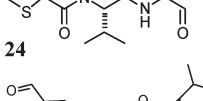
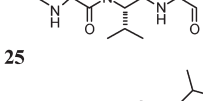
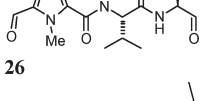
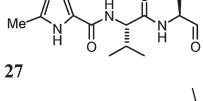
internal contacts. The capping groups all point out of the pocket but in varying positions in relation to the rest of their structure; some are folded back over the dipeptide backbone, some are over Gly208, and others are pointing away from the dipeptide backbone. The variable positioning of the capping groups is consistent with the report that the electron density around the capping group of two α-ketoamide inhibitors was found to be weak within their solved X-ray crystal structures (2R9C and 2R9F), indicating that they are flexible and form limited interactions with the S<sub>3</sub> unprimed region.<sup>38,52</sup> In contrast the Inoue compounds,<sup>40</sup> with the exception of compounds 1, 2, and 11, have a halogen substituent on their capping group with potential to form a hydrogen bond at the P<sub>3</sub> subsite residues Lys347 and Asn253. The other 10 compounds have at least one problem with the required model characteristics required to confer inhibition.

The rationalization of the modeling results with the measured IC<sub>50</sub> values demonstrates the potential ability of the “model” approach to identify potential inhibitors. We now report the results of two modeling studies to confirm the validity of the approach by comparing modeling studies with in vitro experiments.

**Modeling of Acyclic Analogues.** In the first approach we investigated the variation in the capping groups at the P<sub>3</sub> position and assessed whether additional binding could be achieved in the S<sub>3</sub> region for a series of N-heterocyclic analogues of 3. The modeling showed that several of the structures were sufficiently



Table 2. Glide Docking Data for Best Pose of N-Heterocyclic Dipeptides 19–28<sup>b</sup>

Compound	Glide score	Emodel score	Essential H bonds	Warhead distance	Internal contacts			IC <sub>50</sub> (nM)	
					Good	Bad	Ugly	o-CAPN1	o-CAPN2
 <b>19</b>	-6.2	-54.7	3 <sup>a</sup>	3.6	197	20	3	290	25
 <b>20</b>	-5.0	-49.3	3		177	4	2	650	315
 <b>21</b>	-5.0	-52.9	3	4.3	181	5	1	960	100
 <b>22</b>	-5.6	-48.4	3	3.7	173	5	0	790	135
 <b>23</b>	-5.3	-53.8	3	4.1	189	5	0	440	85
 <b>24</b>	-5.0	-46.6	3	3.9	177	3	0	680	100
 <b>25</b>	-5.1	-49.9	3	4.5	184	8	2	530	100
 <b>26</b>	-5.3	-49.9	2 <sup>a</sup>	3.7	199	17	2	150	150
 <b>27</b>	-5.4	-46.7	0	3.5	180	9	0	340	110
 <b>28</b>	-3.2	-49.8	3	3.7	187	6	0	290	140

<sup>a</sup> Hydrogen bonds from the Gly271 carbonyl and Gly208 carbonyl and NH group to the ligand are present but not bonded to the usual ligand donor and acceptor groups of the ligand backbone. <sup>b</sup> Inhibitory concentrations (IC<sub>50</sub>) as previously reported.<sup>53</sup>

promising for us to synthesize 10 N-heterocyclic dipeptides 19–28 and to measure their respective IC<sub>50</sub> values. The Glide docking data for the best pose out of a possible 10 poses generated and kept by Glide and the inhibitory concentrations (IC<sub>50</sub>) against o-CAPN1 and o-CAPN2 for these compounds are shown in Table 2.

The 10 N-heterocyclic dipeptides are all potent or reasonably potent calpain inhibitors, as shown by their low to reasonably low

IC<sub>50</sub> against both o-CAPN2 and o-CAPN1. Compounds 19, 21, and 24 are highly selective for o-CAPN2 over o-CAPN1, while the rest of the compounds display only moderate or little selectivity.<sup>54</sup> The best pose of each of the compounds, excluding 19, 26 and 27, results from docking in an extended  $\beta$ -strand conformation with the three essential hydrogen bonds and with appropriate warhead–nucleophile proximity. Compounds 21–25 have hydrogen bond acceptors in their capping groups

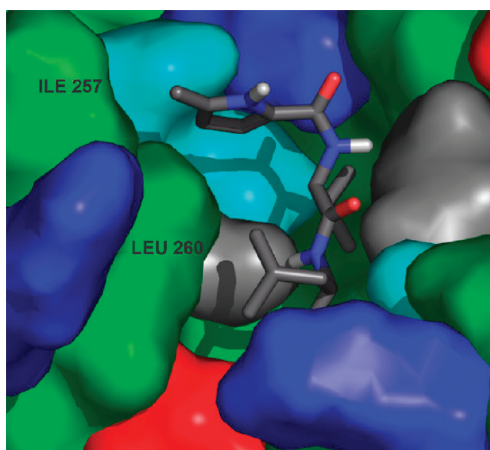


**Figure 13.** Best docked pose of compound **27** (tube structure) from the InducedFit docking. The enzyme is shown as a surface representation with residues color coded by residue property: green = hydrophobic, blue = positive, red = negative, cyan = polar uncharged, gray = glycine.

that form H-bonds with the side chains of either Asn253 or Lys347. These hydrogen bonds are seen in either the best pose of each docked structure or similar poses within the 10 poses collected. Compound **34** has no hydrogen bond acceptor in its capping group, and this may explain its lesser potency against o-CAPN2 and o-CAPN1.

Compound **27** docks in an appropriate manner but only using an InducedFit protocol. Like compound **20** it has no hydrogen bond acceptors in its capping group. The 5-methylpyrrole capping group is uniquely twisted, and the methyl group is pointing into a hydrophobic pocket formed by the enzyme residues Ile257 and Leu260 giving rise to a hydrophobic–hydrophobic interaction (Figure 13). This interaction can explain why **27** is more potent than compound **20**, which does not have the hydrophobic methyl group. The methoxycarbonylpyrrole group of compound **28** has the potential to form hydrogen bonds with the likes of Lys347 and Asn253, but no such interactions were observed in any of the poses. The poses have the compound docking in a mode similar to that of compound **26**.

The 10 compounds showed varying degrees of potency and selectivity, although the differences are not large. Most of the compounds' best docked poses exhibited the potential to form hydrogen bonds with the residues surrounding the S<sub>3</sub> subsite of the enzyme and exhibited the substrate in a  $\beta$ -strand with an appropriate distance of the warhead to the cysteine sulfur.

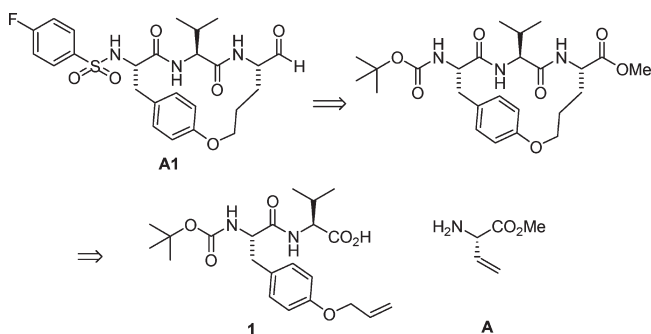
Compound **19** has a distinctive binding mode, and compound **28** also showed this mode in some poses. This latter binding mode exhibits the potential to form hydrogen bonds between the pyrrole aldehyde and surrounding residues such as Lys347. If this unusual binding mode is in fact the actual manner in which it binds, then it alone could account for the increased potency.<sup>55</sup> Using the InducedFit docking protocol did not add anything to the results of the Glide docking except in the case of compound **27**, which did not dock appropriately with Glide but did produce a viable pose using the InducedFit protocol. Therefore, it may be necessary to use the more expensive InducedFit protocol in cases when Glide does not produce appropriate docked poses.

**Modeling of Macrocyclic Analogues.** The second class of compounds investigated were macrocycles that were studied to establish whether we could constrain our lead compound **3** as a macrocycle so that the amino acid segment of the molecule is

constrained as a  $\beta$ -strand and such to position functional groups appropriately for binding with calpain. This follows from Fairlie's analysis of the importance of a  $\beta$ -strand for bioactivity. Fairlie has reported that incorporating a tripeptide into a  $\sim$ 17-membered ring can favor a tripeptide in an extended  $\beta$ -strand conformation.<sup>56,57</sup> Our aim has been to constrain the calpain inhibitor molecule into a bioactive conformation, thereby lowering the entropic barrier for binding to calpain.

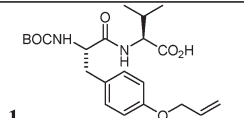
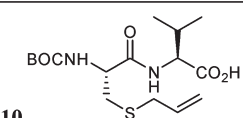
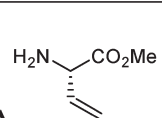
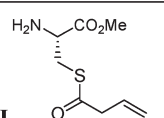
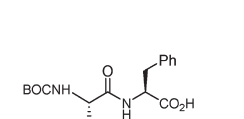
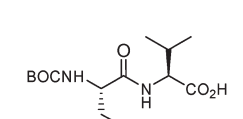
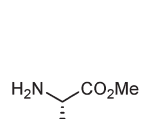
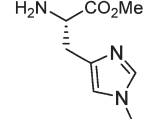
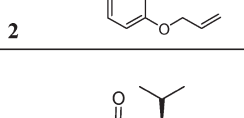
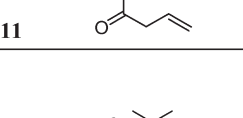
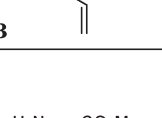
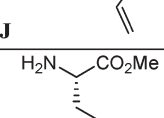
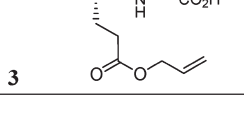
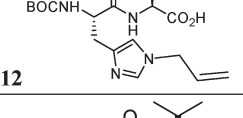
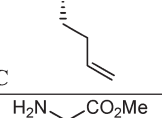
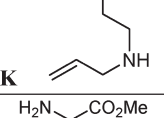
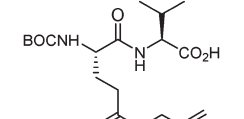
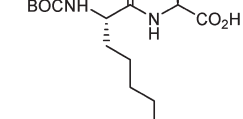
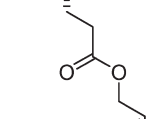
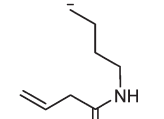
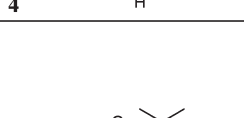
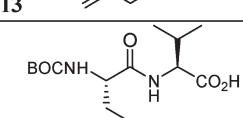
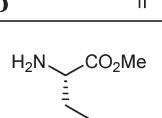
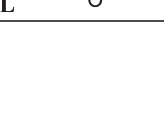
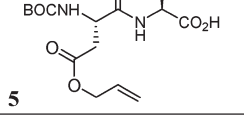
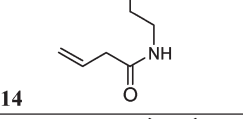
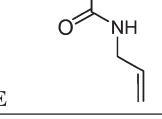
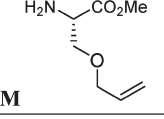
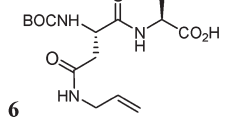
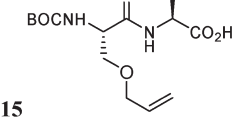
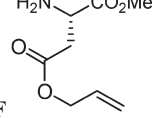
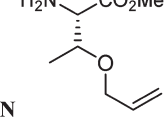
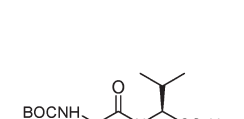
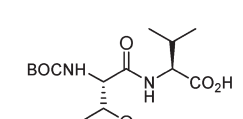
A library of possible candidate molecules was developed, but a criterion for selection into the library was that a synthetic route to each structure was feasible. The library was constructed from an 18  $\times$  16 grid matrix shown in Table 3, yielding 288 possible tripeptide macrocyclic structures. A generic synthetic route for each macrocycle involves an *N*-BOC-allyl-amino acid with an olefin in the side chain (left columns Table 3) being coupled with an allylamino acid methyl ester also with an olefin in the side chain (right columns Table 3) to yield the corresponding acyclic diene. Ring closing metathesis, a proven route to macrocyclization, could be used to form each macrocycle.<sup>58</sup> We have subsequently explored other routes that have proved to be more amenable to large scale production of compounds that have been shown to be of particular commercial interest.<sup>59</sup>

For example, **A1** is the 4-fluorobenzylsulfonamide protected aldehyde that results from reaction of *N*-BOC-allylamino acid **1** and allylamino acid methyl ester **A** and involves ring closing metathesis and replacement of the Boc group with fluorosulfonate and modification of the ester to aldehyde. The 288 possible core structures developed by combination of the structures in Table 3 can be extended to contain different capping warhead and core groups. For the initial study the warhead for each of the 288 structures was an aldehyde, and the protecting group was 4-fluorobenzylsulfonamide.<sup>60</sup>



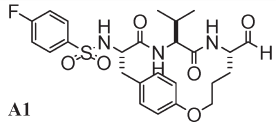
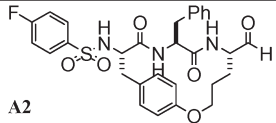
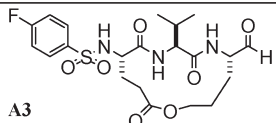
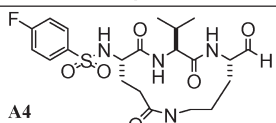
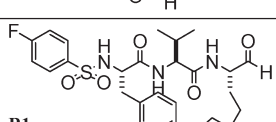
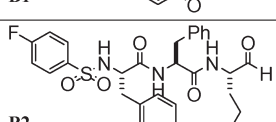
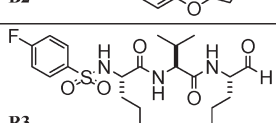
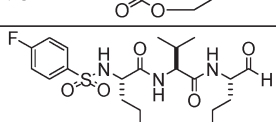
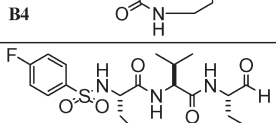
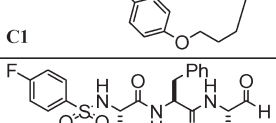
A sample of 10<sup>54</sup> compounds **A1–4**, **B1–4**, **C1**, and **C2** were docked into the enzyme model using both Glide and InducedFit protocols, and the results showed that some of the structures could dock into the active site in a fashion that indicated their potential to be good inhibitors while others failed to dock appropriately. This can sometimes be because inappropriate starting conformations were used. The structures that did not dock appropriately in the first instance were redocked using the lowest energy  $\beta$ -strand conformation, and often this proved to result in appropriate poses. However, some of the 10 structures were docked with poses that did not meet the criteria of (i) having the three essential H-bonds, (ii) close warhead–nucleophile distance, and (iii) low Glide and Emodel scores. From this study the InducedFit protocol was identified as more a more satisfactory protocol, though more expensive, as it allowed some movement of the enzyme active site and was used in subsequent studies (Table 4).

**Table 3. Acids 1–18 Coupled with Esters A–P and Closed by Ring Closing Metathesis Gives an in Silico Library of 288 Macrocyclic Tripeptides<sup>a</sup>**

N-BOC-allyl-amino acid		Allyl-amino acid methyl ester	
 <b>1</b>	 <b>10</b>	 <b>A</b>	 <b>I</b>
 <b>2</b>	 <b>11</b>	 <b>B</b>	 <b>J</b>
 <b>3</b>	 <b>12</b>	 <b>C</b>	 <b>K</b>
 <b>4</b>	 <b>13</b>	 <b>D</b>	 <b>L</b>
 <b>5</b>	 <b>14</b>	 <b>E</b>	 <b>M</b>
 <b>6</b>	 <b>15</b>	 <b>F</b>	 <b>N</b>
 <b>7</b>	 <b>16</b>	 <b>G</b>	 <b>O</b>
 <b>8</b>	 <b>17</b>	 <b>H</b>	 <b>P</b>
 <b>9</b>	 <b>18</b>		

<sup>a</sup> These are modified in silico to give the equivalent 4-fluorobenzylsulfonamide protected aldehydes to give compounds labeled A1, A2, A3, ..., P16, P17, P18.

Table 4. Docking Data for Best Pose<sup>a</sup> (Out of Possible 20) for Compounds A1–4, B1–4, C1, and C2 for InducedFit Docking<sup>c</sup>

Compound	Ring size	% <sup>b</sup> $\beta$ -strand	Glide Score	Emodel Score	Essential H bonds	Warhead Distance Å	Internal contacts			IC <sub>50</sub> (nM) CAPN2
							Good	Bad	Ugly	
 A1	16	100	-7.4	-84.0	3	4.2	217	17	0	3710
 A2	16	100	-7.4	-67.8	2	>5	274	26	0	
 A3	14	16	-6.7	-77.3	3	3.8	254	8	0	
 A4	14	50	-8.8	-77.3	3	4.9	258	5	0	
 B1	17	57	-8.1	-53.5	3	3.9	287	16	1	280
 B2	17	27	-7.0	-88.7	0	>5	287	21	0	
 B3	15	8	-7.9	-69.0	3	4.4	261	10	1	
 B4	15	6	-7.6	-81.6	0	>5	292	4	0	
 C1	18	53	-6.0	-77.2	0	>5	300	18	0	
 C2	18	16	-6.4	-78.6	3	4.1	307	31	6	

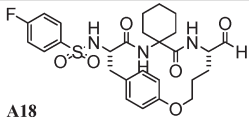
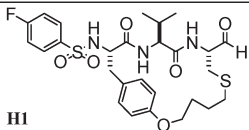
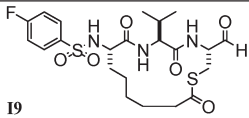
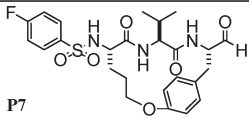
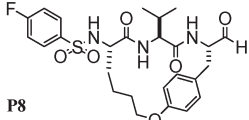
<sup>a</sup> Best pose chosen by criteria in order of importance: 1, presence of three essential hydrogen bonds; 2, warhead within 5 Å of nucleophilic Cys115; 3, low Glide score/emodel score; 4, lowest number of internal ugly contacts. <sup>b</sup> Percentage of the ensemble in a  $\beta$ -strand. <sup>c</sup> IC<sub>50</sub> data as reported previously.<sup>61</sup>

The ensembles of low energy conformers of the compounds in Table 4 in the absence of the enzyme were mixtures of  $\beta$ -strand and turn-type conformations, and those that docked well exhibited a propensity for a  $\beta$ -strand conformation in the ensemble of conformers of the starting compounds.

To select structures for further investigation, we therefore first undertook conformational searches of all 288 compounds to establish their propensity for  $\beta$ -strand conformations and from this analysis made a selection of structures for docking studies.<sup>62,54</sup> Docking results of five fluorosulfonate compounds



Table 5. Docking Data for Best Pose (Out of Possible 20) for Compounds A18, H1, I9, P7, and P8<sup>b</sup>

Compound	Ring size	% <sup>a</sup> $\beta$ -strand	Glide Score	Emodel Score	Essential H bonds	Warhead Distance Å	Internal contacts			IC <sub>50</sub> (nM) CAPN2
							Good	Bad	Ugly	
 <b>A18</b>	16	98	-6.4	-69.6	2	3.5	378	31	13	
 <b>H1</b>	19	95	-7.6	-87.3	3	3.5	295	15	0	2400
 <b>I9</b>	15	98	-6.9	-68.5	3	3.5	271	7	1	
 <b>P7</b>	16	92	-5.1	-71.9	3	3.8	285	11	0	
 <b>P8</b>	17	94	-8.0	-70.2	3	4.0	291	12	0	

<sup>a</sup> Percentage of the ensemble in a  $\beta$ -strand. <sup>b</sup> IC<sub>50</sub> data as reported in literature.<sup>61</sup>

A18, H1, I9, P7, and P8 with a high propensity for a  $\beta$ -strand are shown in Table 5 (A1 and A2 also exhibit a high propensity for a  $\beta$ -strand and are shown in Table 4). With the exception of A2 all exhibited good docking characteristics using the InducedFit Protocol. H1, A1 (Table 5),<sup>63</sup> and B1 (Table 4) were subsequently synthesized and exhibited IC<sub>50</sub> values of 2400, 3710, and 280 nM, respectively.

To examine if we could increase the potency of the macrocycles, the cores of compounds A1, B1, C1, and H1 were used as templates and the capping group, the P<sub>2</sub> side chain, and the warhead were varied. These four templates were chosen because compounds A1, B1, and H1 once synthesized turned out to be inhibitors of calpain to varying degrees and C1 is an analogous molecule to A1 and B1 but with a larger macrocyclic ring. We decided to replace the 4-fluorobenzenesulfonamide with a Cbz group in an attempt to increase bioavailability and potency and to vary the alkyl group at the P<sub>2</sub> position.<sup>64</sup> We showed above that phenylalanine at the P<sub>2</sub> position is too large to fit into the deep hydrophobic pocket of the S<sub>2</sub> subsite. Leucine, which is larger than valine but smaller than phenylalanine, is a hydrophobic amino acid and was also investigated at the P<sub>2</sub> position. We also wanted to examine the effect of ring size.

We report on 12 structures, namely, 29, 32, 35, and 38, 30, 33, 36, and 39 along with the alcohols 31, 34, 37, and 40 (Table 6). The latter four alcohols were included in the study in order to establish if the alcohol could function as a warhead, since aldehydes are reactive and can react with other cellular proteins.<sup>65</sup> An alcohol can mimic the tetrahedral intermediate formed when

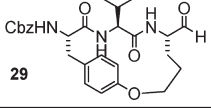
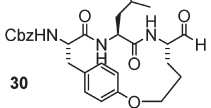
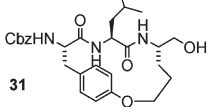
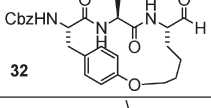
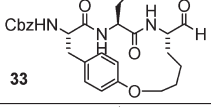
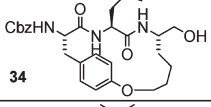
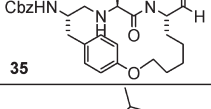
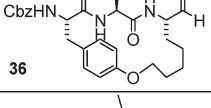
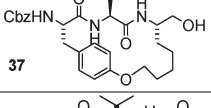
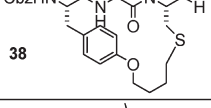
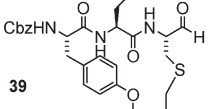
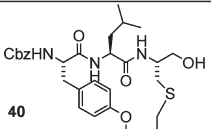
the aldehyde reacts with the active site cysteine of calpain, as is seen in X-ray structures such as 2G8E.<sup>37</sup> Although such compounds could not form a reversible covalent bond with the active site cysteine of calpain, the molecules do not react so readily with other proteins in a biological system and were therefore included in the investigation. The Boltzmann weighted percentage of conformers within a 12 kJ window displaying a  $\beta$ -strand conformation for each structure along with the macrocycle ring size for each is shown in Table 5.

Ten of these compounds have now been synthesized,<sup>66</sup> and the IC<sub>50</sub> values of these are shown in Table 6 along with the results of the docking studies. Compounds 29 and 35 were not synthesized. All 12 compounds were docked into the enzyme model with the InducedFit protocol (Table 5), and with the exception of 40 all were docked in an appropriate manner. Compound 40 was not expected to dock, as the Boltzmann weighted percentage of conformers in a  $\beta$ -strand was calculated at zero percent, indicative that it could not adopt the bioactive conformation without a considerable cost in energy.

Compounds 29, 32, 35, and 38 are Cbz protected aldehyde macrocycles with valine at the P<sub>2</sub> position. Compounds 30, 33, 36, and 39 are analogues of 29, 32, 35, and 38, with valine at the P<sub>2</sub> replaced by leucine. The docking of 30, 33, 36, and 39 provides strong evidence that leucine at the P<sub>2</sub> position could comfortably dock into the S<sub>2</sub> subsite.

Ten of these 12 structures (not 29 and 35) were synthesized and tested in vitro. Compound 40 was synthesized to see if the modeling correctly predicted that it would not be a good

Table 6. Docking Data for Best Pose<sup>a</sup> (Out of Possible 20) for Compounds 4.9–4.20<sup>c</sup>

Structure	Ring size	% <sup>b</sup> $\beta$ -strand	Glide Score	Emodel Score	Essential H bonds	Warhead Distance Å	Internal contacts			IC <sub>50</sub> (nM) CAPN2
							Good	Bad	Ugly	
 <b>29</b>	16	99	-8.3	-71.3	3	3.4	277	17	1	
 <b>30</b>	16	100	-8.4	-86.6	3	3.7	307	22	2	850
 <b>31</b>	16	99	-9.7	-83.7	3	NA	311	26	5	31000
 <b>32</b>	17	65	-8.0	-78.1	3	3.9	280	18	1	85
 <b>33</b>	17	8	-4.5	-67.3	3	4.0	309	20	1	30
 <b>34</b>	17	75	-9.0	-77.5	3	NA	340	24	2	700
 <b>35</b>	18	89	-7.8	-84.9	3	4.1	303	18	0	
 <b>36</b>	18	85	-10.0	-69.1	3	4.0	325	14	3	180
 <b>37</b>	18	53	-10.1	-82.8	3	NA	313	21	1	1100
 <b>38</b>	19	35	-9.2	-87.5	3	4.2	285	14	1	295
 <b>39</b>	19	39	-9.7	-66.4	3	4.8	314	21	2	1010
 <b>40</b>	19	0	-9.4	-79.3	0	NA	347	26	8	28,000

<sup>a</sup> Best pose chosen by criteria in order of importance: 1, presence of three essential hydrogen bonds; 2, warhead within 5 Å of nucleophilic Cys115; 3, low Glide score/emodel score; 4, lowest number of internal ugly contacts. <sup>b</sup> Percentage of the ensemble in a  $\beta$ -strand. <sup>c</sup> Inhibitory concentrations (IC<sub>50</sub>) as reported<sup>66</sup> and for **32** and **38** in a patent.<sup>61</sup>

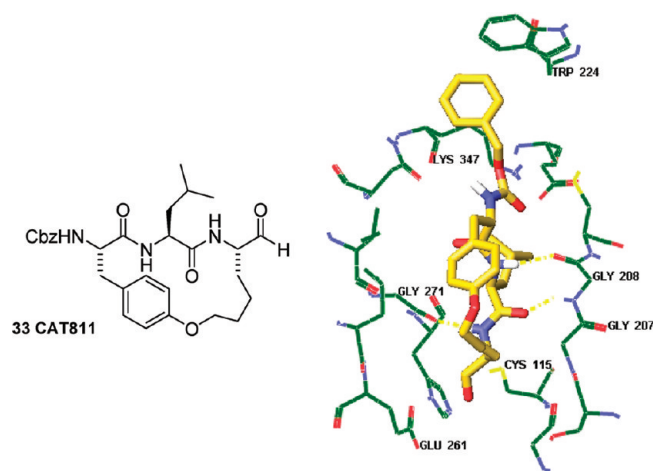


Figure 14. Macrocycle 33 and its best docked pose.

inhibitor of CAPN2, and this proved to be correct as illustrated by the high  $IC_{50}$  of 28 000 nM. All the other tested compounds, except 31, proved to be at least moderately good inhibitors, and 32, 33, 36, and 38 turned out to be excellent inhibitors with  $IC_{50}$  of 85, 30 180, and 295 nM, respectively. The larger leucine side chain, compared to valine, at the  $P_2$  position fits into the deep hydrophobic pocket of the  $S_2$  subsite. Changing a valine in 32 to a leucine 33 had a positive effect on the  $IC_{50}$ , and this molecule possessed an optimal macrocyclic ring size of 17 (Figure 14).

The low  $IC_{50}$  of 33 (also known as CAT811) in the *in vitro* experiment led us to undertake an *in vivo* experiment to determine whether 33 could retard the development of calcium-induced cortical cataracts in cultured ovine lenses.<sup>3</sup> Lenses treated with calcium only showed substantial opacity characteristic of cataract formation. The presence of 1  $\mu$ M compound 33 in the culture medium prevented this calcium-induced opacification, and the lenses remained essentially transparent after incubation for 6 h in the culture medium. Thus, compound 33 was able to significantly reduce the onset of lens opacity.<sup>66</sup>

Compounds 31, 34, 37, and 40 are analogues of 30, 33, 36, and 39, with the aldehyde replaced with alcohol. Cysteine proteases have been problematic for drug design, as many of the known inhibitors contain an electrophilic “warhead” that binds covalently in a reversible or irreversible manner, making the inhibitor particularly reactive such that they can bind nonspecifically to proteins, receptors, and biomolecules *in vivo*. This can give rise to problems with toxicity associated with drug metabolism and pharmacokinetics.<sup>67</sup> There is therefore interest in developing selective inhibitors that can address such problems. The problem is somewhat reduced for the treatment of cataract, as application can be directly to the eye. Because aldehydes are known to react with other molecules under cellular conditions, it was hoped that changing the warhead to an alcohol would still facilitate the inhibition of calpain by mimicking the tetrahedral intermediate which is stabilized by H-bonds in the oxyanion hole. The alcohols were therefore included in the study in order to establish the extent to which an alcohol might mimic the tetrahedral intermediate formed when the aldehyde reacts covalently and reversibly with the active site cysteine of calpain as is seen in X-ray structures such as 2G8E.<sup>68</sup> Although these alcohols cannot form a reversible covalent bond with the active site cysteine of calpain, the fact that they do not react promiscuously with other cellular proteins as do their aldehyde analogues could offer advantage.

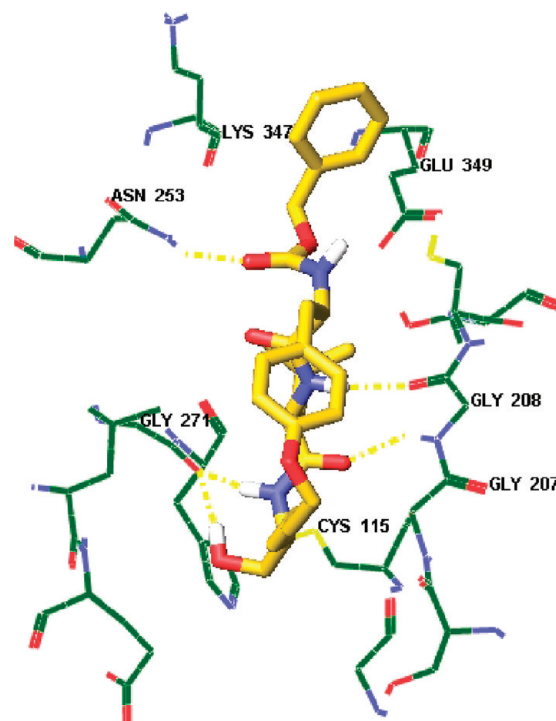


Figure 15. Best docked poses 4,14 using the InducedFit protocol.

If the respective  $IC_{50}$  values are not equivalent to their aldehyde counterparts, hopefully the trade-off in potency would offset the aldehydes' innate reactivity to other proteins under cellular conditions. The modeling results showed that compounds 34 and 37 were acceptable and potential candidate calpain inhibitors with all the essential criteria for inhibition. The compounds were prepared and were moderately good inhibitors but 1–2 orders of magnitude less potent than their aldehyde counterparts 33 and 36. To date, the molecules have yet to be tested *in vivo* to establish whether the trade-off in potency is overcome by the proposed reduction in their tendency to react with other cellular proteins.

Compound 34 has an  $IC_{50}$  of 700 nM, which is acceptable considering it has an alcohol in place of the usual aldehyde warhead. The alcohol forms a H-bond with the side chain of Gly271 (Figure 15) and is unexpectedly pointing away from the oxyanion hole (usually formed by two stabilizing H-bonds, one between the oxyanion of a tetrahedral intermediate and the backbone NH of Cys115 and the other between the oxyanion and the side chain of Gln109).<sup>37</sup> Compound 31 satisfied the main docking criteria, but the best poses had a high number of “ugly” internal contacts and the compound has a poor  $IC_{50}$  of 31 000 nM. The conformational search results of 40 showed that it did not form a  $\beta$ -strand. The lowest energy conformer of the compound, a turn type conformation, was docked with the predictable outcome that it could not dock with the required criteria and was a poor inhibitor of calpain exhibiting a  $IC_{50}$  of 28 000 nM.<sup>54</sup>

## CONCLUSION

Modeling studies have been validated as a valuable tool to identify those compounds to select from an extensive library to synthesize molecules that have calpain inhibitory properties. The docking modeling approach also provides a rationale for the

modification of the core template of macrocycles with the objective of designing more sophisticated and potent inhibitors of CAPN2.<sup>69</sup> Progress in the field will be accelerated by the availability of faster computers and algorithms that will increase the speed of the necessary computations. In this study, modeling has provided a valuable tool for the rational design of the molecule **33** which slows cataractogenesis and consequently is a drug candidate to retard cataract formation. Indeed **33** is the most potent compound we have prepared with an in vitro IC<sub>50</sub> of 30 nM, and when tested in an in vitro ovine culture lens system, it significantly retarded the formation of cortical cataracts in ovine lenses.

## EXPERIMENTAL SECTION

**Conformational Search Method.** Conformational searches were carried out with MacroModel, version 9.1,<sup>70</sup> to generate an ensemble of low energy conformers. The searches were conducted with the MCMM method using a GB/SA water model and the OPLS2001 force field, with 3000 steps for the conformational search and up to 5000 iterations for the minimization of each generated structure. The minimization was stopped with the default gradient convergence threshold of  $\delta = 0.05$  kJ/(mol·Å). The default Polak–Ribiere conjugate gradient method was used for all minimizations.

**Refinement of the Glide and InducedFit Model from 1KXR.** The crystal structure of mini  $\mu$ -calpain (PDB code 1KXR)<sup>25</sup> was prepared by deleting waters and ions and mutation of Ser115 to Cys115. This structure was minimized using the OPLS2001 force field with a GB/SA water model with over 500 iterations. All residues within a 5 Å distance to the calcium ions of the crystal structure were kept frozen during this minimization. The rmsd of the minimized structure to the crystal structure was 0.96 Å for the heavy atoms (C, N, O, S). The structure was refined by the Prime preparation and refinement tool. The cysteine sulfur of Cys115 was deprotonated.

**Glide Docking Protocol.** For grid generation, the center of the docking grid was defined as the centroid of the residues Cys115, Gly208, Gly271, and Lys347 and was generated with Glide, version 4.0,<sup>71</sup> using default settings. The midpoint of each docked ligand was set to a 12 Å × 12 Å × 12 Å box. van der Waals radii of the receptor atoms were scaled to 1.0. All other settings were default settings.

**Ligand Docking.** Ligands were docked flexibly in extra precision mode (XP) and with a van der Waals scaling of 0.8. The structure output was set to write out 10 or 20 poses per ligand. All other settings were default settings.

**InducedFit Docking Protocol.** The InducedFit docking script<sup>72</sup> using Prime and Glide was opened in Maestro. For the Glide enclosing box, the center of the docking grid was defined as the centroid of the residues Cys115, Gly208, Gly271, and Lys347. The size was set at auto. Step 1, protein preparation constrained refinement, involved removal of side chain of Lys347 and extra precision (XP) mode; all other settings were at default. Step 2 used default settings. Step 3 used extra precision (XP) mode. All other settings were at default.

**Synthesis.** The compounds where IC<sub>50</sub> data are reported were prepared as referenced in the tables.<sup>53,61,66</sup> Elemental analytical data, high resolution mass spectra, and IC<sub>50</sub> data are as published. The compounds are >95% pure. Elemental analysis and high resolution mass spectrometry are used to establish purity as recorded in the publications. Unless otherwise stated in the papers or in their corresponding supplementary material, purification was by column or flash chromatography in conjunction with thin layer chromatography. Data in Table 1 are from the literature,<sup>40</sup> and the supplementary material to those papers indicates that each compound has satisfactory elemental analysis results.

**Bodipy Assay.** The biological activity of the calpain inhibitors was determined by measuring the inhibition constants (IC<sub>50</sub>) in an in vitro

assay. The testing was performed in the Lincoln University research laboratory, and an established assay protocol was used by Dr. Janna Nikkel. This assay utilized a quenched fluorogenic substrate, casein labeled with the fluorophore 4,4-difluoro-5,7-dimethyl-4-bora-3a,4a-diaza-s-indacene-3-propionic acid (BODIPY).<sup>73</sup> Fluorescence increases as proteolysis of the substrate occurs.

## AUTHOR INFORMATION

### Corresponding Author

\*For J.M.C.: phone, +64 3 3642872; e-mail, Jim.Coxon@Canterbury.ac.nz. For J.D.M.: phone, +64 3 3253838 Extn 8169; e-mail, Jim.Morton@Lincoln.ac.nz.

### Present Addresses

<sup>||</sup>University of Adelaide, Adelaide, Australia.

## ACKNOWLEDGMENT

We gratefully acknowledge a grant from the Foundation for Research Science and Technology of New Zealand (Grants LINX0205 and LINX03007), the Auckland Centre for Molecular Biodiscovery, and Douglas Pharmaceuticals Ltd. for student support.

## ABBREVIATIONS USED

CAPN1, calpain 1 or  $\mu$ -calpain; CAPN2, calpain 2 or  $m$ -calpain; o-CAPN1, ovine calpain 1; o-CAPN2, ovine calpain 2

## REFERENCES

- (1) Duncan, G.; Bushell, A. R. Ion Analyses of Human Cataractous Lenses. *Exp. Eye Res.* **1975**, *20*, 223–230. Duncan, G.; Jacob, T. J. C. Calcium and the Physiology of Cataract. *CIBA Found. Symp.* **1984**, *106*, 132–148.
- (2) Sanderson, J.; Marcantonio, J. M.; Duncan, G. Calcium Ionophore Induced Proteolysis and Cataract: Inhibition by Cell Permeable Calpain Antagonists. *Biochem. Biophys. Res. Commun.* **1996**, *218*, 893–901.
- (3) Lee, H. Y.; Morton, J. D.; Sanderson, J.; Bickerstaffe, R.; Robertson, L. The Involvement of Calpains in Opacification Induced by Ca<sup>2+</sup>-Overload in Ovine Lens Culture. *Vet. Ophthalmol.* **2008**, *11*, 347–355.
- (4) Robertson, L. J. G.; Morton, J. D.; Yamaguchi, J. M.; Bickerstaffe, R.; Shearer, T. R.; Azuma, M. Calpain May Contribute to Hereditary Cataract Formation in Sheep. *Invest. Ophthalmol Visual Sci.* **2005**, *46*, 4634–4640.
- (5) Dutt, P.; Spriggs, C. N.; Davies, P. L.; Jia, Z.; Elce, J. S. Origins of the Difference in Ca<sup>2+</sup> Requirement for Activation of  $\mu$ - and  $m$ -Calpain. *Biochem. J.* **2002**, *367*, 263–269. Moldoveanu, T.; Gehring, K.; Green, D. R. Concerted Multipronged Attack by Calpastatin To Occlude the Catalytic Cleft of Heterodimeric Calpains. *Nature* **2008**, *456*, 404–408. Hanna, R. A.; Campbell, R. L.; Davies, P. L. Calcium-Bound Structure of Calpain and Its Mechanism of Inhibition by Calpastatin. *Nature* **2008**, *456*, 409–412. Blanchard, H.; Grochulski, P.; Li, Y.; Arthur, J. S. C.; Davies, P. L.; Elce, J. S.; Cygler, M. Structure of a Calpain Ca<sup>2+</sup> Binding Domain Reveals a Novel EF-Hand and Ca<sup>2+</sup>-Induced Conformational Changes. *Nat. Struct. Biol.* **1997**, *4*, 532–538. Davies, T. L.; Walker, J. R.; Finerty, P. J., Jr.; Mackenzie, F.; Newman, E. M.; Dhe-Paganon, S. The Crystal Structure of Human Calpains 1 and 9 Imply Diverse Mechanisms of Action and Autoinhibition. *J. Mol. Biol.* **2007**, *366*, 216–229. Li, Q.; Hanzlik, R. P.; Weaver, R. F.; Schoenbrunn, E. Molecular Mode of Action of a Covalently Inhibiting Peptidomimetic on the Human Calpain Protease Core. *Biochemistry* **2006**, *45*, 701–708. Cuerrier, D.; Moldoveanu, T.; Campbell, R. L.; Kelly, J.; Yoruk, B.; Verhelst, S. H. L.; Greenbaum, D.; Bogoy, M.; Davies, P. L. Development of Calpain-



Specific Inactivators by Screening of Positional Scanning Epoxide Libraries. *J. Biol. Chem.* **2007**, *282*, 9600–9611. Quian, J.; Cuerrier, D.; Davies, P. L.; Li, Z.; Powers, J. C.; Campbell, R. L. Cocystal Structures of Primed Side-Extending  $\alpha$ -Ketoamide Reveal Novel Calpain-Inhibitor Aromatic Interactions. *J. Med. Chem.* **2008**, *51*, S264–S270.

(6) Fukiage, C.; Nakajima, E.; Ma, H.; Azuma, M.; Shearer, R. Characterization and Regulation of Lens-Specific Calpain Lp82. *J. Biol. Chem.* **2002**, *277*, 20678–20685.

(7) Goll, D. E.; Thompson, V. F.; Li, H.; Wei, W.; Cong, J. The Calpain System. *Physiol. Rev.* **2003**, *83* (3), 731–801.

(8) Basak, A.; Bateman, O.; Slingsby, C.; Pande, A.; Asherie, N.; Ogun, O.; Benedek, G. B.; Pande, J. High-resolution X-ray Crystal Structures of Human  $\gamma$ D Associated with Aculeiform Cataract. *J. Mol. Biol.* **2003**, *328*, 1137–1147.

(9) Purkiss, A. G.; Bateman, O.; Goodfellow, J. M.; Lubsen, N. H.; Slingsby, C. The X-ray Crystal Structure of Human  $\gamma$ S-Crystallin C-Terminal Domain. *J. Biol. Chem.* **2002**, *277*, 4199–4205.

(10) Lampi, K. J.; Ma, Z.; Hanson, S. R. A.; Azuma, M.; Shih, M.; Shearer, T. R.; Smith, D. L.; Smith, J. B.; David, L. L. Age Related Changes in Human Lens Crystallins Identified by Two-Dimensional Electrophoresis and Mass Spectrometry. *Exp. Eye Res.* **1998**, *67*, 31–43.

(11) Srivastava, O. P.; Srivastava, K. Degradation of  $\gamma$ D- and  $\gamma$ S-Crystallins in Human Lenses. *Biochem. Biophys. Res. Commun.* **1998**, *253*, 288–294.

(12) Srivastava, O. P.; Srivastava, K.  $\beta$ B2-Crystallin Undergoes Extensive Truncation during Aging in Human Lenses. *Biochem. Biophys. Res. Commun.* **2003**, *301*, 44–49.

(13) Hanson, S. R. A.; Hasan, A.; Smith, D. L.; Smith, J. B. The Major in Vivo Modifications of the Human Water-Insoluble Lens Crystallins Are Disulfide Bonds, Deamidation, Methionine Oxidation and Backbone Cleavage. *Exp. Eye Res.* **2000**, *71*, 195–207.

(14) Ueda, Y.; Fukiage, C.; Shih, M.; Shearer, T. R.; David, L. L. Mass Measurements of C-Terminally Truncated  $\alpha$ -Crystallins from Two-Dimensional Gels Identify Lp82 as a Major Endopeptidase in Rat Lens. *Mol. Cell. Proteomics* **2002**, *1*, 357–365.

(15) Lund, A. L.; Smith, J. B.; Smith, D. L. Modifications of the Water-Insoluble Human Lens  $\alpha$ -Crystallins. *Exp. Eye Res.* **1996**, *63*, 661–672.

(16) Calpains belong to the largest clan of cysteine proteases, clan CA, a clan that contains half of all cysteine protease families. Cysteine proteases typically have an active site consisting of a catalytic diad containing a cysteine and a histidine. Barrett, A. J.; Rawlings, N. D. Evolutionary Lines of Cysteine Peptidases. *Biol. Chem.* **2001**, *382*, 727–733. Calpain itself has a catalytic triad that contains cysteine, histidine, and an asparagine. In mammals there are various isoforms found. Some are tissue specific, and others have been isolated from almost all tissue types. Some tissue specific calpains include p94 (skeletal muscle), Lp82 (lens), nCL-2 (stomach), nCL-4 (digestive organ), and CAPN6 (placenta). The ubiquitous calpains CAPN1 and CAPN2 are well characterized. They require micromolar and millimolar  $\text{Ca}^{2+}$  concentrations, in vitro, for activation, respectively.

(17) Macqueen, D. J.; Delbridge, M. L.; Manthri, S.; Johnston, I. A. A Newly Classified Vertebrate Calpain Protease, Directly Ancestral to CAPN1 and 2, Episodically Evolved a Restricted Physiological Function in Placental Mammals. *Mol. Biol. Evol.* **2010**, *27* (8), 1886–1902.

(18) Toh, T.Y.; Morton, J.; Coxon, J. M.; Elder, M. J. Medical Treatment of Cataract. *Clin. Exp. Ophthalmol.* **2007**, *35*, 664–671.

(19) Todd, B.; Moore, D.; Deivanayagam, C. C. S.; Lin, G.; Chattopadhyay, D.; Maki, M.; Wang, K. K. W.; Narayana, S. V. L. A Structural Model for the Inhibition of Calpain by Calpastatin: Crystal Structures of the Native Domain VI of Calpain and Its Complexes with Calpastatin Peptide and a Small Molecule Inhibitor. *J. Mol. Biol.* **2003**, *No. 328*, 131–146.

(20) Reverter, D.; Braun, M.; Fernandez-Catalan, C.; Strobl, S.; Sorimachi, H.; Bode, W. Flexibility Analysis and Structure Comparison of Two Crystal Forms of Calcium-Free Human m-Calpain. *Biol. Chem.* **2002**, *383*, 1415–1422.

(21) Blanchard, H.; Grochulski, P.; Li, Y.; Arthur, J. S. C.; Davies, P. L.; Elce, J. S.; Cygler, M. Structure of a Calpain  $\text{Ca}^{2+}$ -Binding Domain

Reveals a Novel EF-H and  $\text{Ca}^{2+}$ -Induced Conformational Changes. *Nat. Struct. Biol.* **1997**, *4*, 532–538. The structures were not of the complete enzyme but of the  $\text{Ca}^{2+}$ -binding domain VI of rat CAPN2 in the absence of  $\text{Ca}^{2+}$  (PDB code 1AJ5) and with  $\text{Ca}^{2+}$  bound (1DVI). The X-ray structures revealed that domain VI contained five EF-hand motifs and that three of them are bound to  $\text{Ca}^{2+}$ . EF-hands are helix–loop–helix structural motifs that are known to commonly bind  $\text{Ca}^{2+}$ . The presence of structural changes induced by  $\text{Ca}^{2+}$  binding at the EF-hands gave critical insights into how  $\text{Ca}^{2+}$  binding causes activation of calpain.  $\text{Ca}^{2+}$  binds to domain VI and the structurally similar domain IV and induces the structural changes in the active site that are necessary for activation of the enzyme. The first crystal structure of an entire calpain heterodimer was reported by Hosfield. Hosfield, C. M.; Elce, J. S.; Davies, P. L.; Jia, Z. Crystal Structure of Calpain Reveals the Structural Basis for  $\text{Ca}^{2+}$  Dependent Protease Activity and a Novel Mode of Enzyme Activation. *EMBO J.* **1999**, *18*, 6880–6889. The structure was of rat CAPN2 in the absence of  $\text{Ca}^{2+}$  (1DFO) and confirmed for the first time that the catalytic triad was not in an active conformation when  $\text{Ca}^{2+}$  was absent. This structure 1DFO was followed by the publication of two structures of human CAPN2 (1KFU and 1KFX) both in the absence of  $\text{Ca}^{2+}$ , and these confirmed the existence of a disrupted active site for the apoenzyme. Strobl, S.; Fernandez-Catalan, C.; Braun, M.; Huber, R.; Masumoto, H.; Nakagawa, K.; Irie, A.; Sorimachi, H.; Bourenkowi, G.; Bartuniki, H.; Suzuki, K.; Bode, W. The Crystal Structure of Calcium-Free Human m-Calpain Suggests an Electrostatic Switch Mechanism for Activation by Calcium. *Proc. Natl. Acad. Sci. U.S.A.* **2000**, *97*, 588–592.

(22) Berman, H. M.; Westbrook, J.; Feng, Z.; Gilliland, G.; Bhat, T. N.; Weissig, H.; Shindyaov, I. N.; Bourne, P. E. The Protein Data Bank. *Nucleic Acids Res.* **2000**, *28*, 235–242.

(23) Gabrijelcic-Geiger, D.; Mentele, R.; Meisel, B.; Hinz, H.; Assfalg-Machleidt, I.; Machleidt, W.; Möller, A.; Auerswald, E. A. Human  $\mu$ -Calpain: Simple Isolation from Erythrocytes and Characterization of Autolysis Fragments. *Biol. Chem.* **2001**, *382*, 173–1737.

(24) Pietsch, M.; Chua, K. C. H.; Abell, A. D. Calpains: Attractive Targets for the Development of Synthetic Inhibitors. *Curr. Top. Med. Chem.* **2010**, *10*, 270–293.

(25) Moldoveanu, T.; Hosfield, C. M.; Lim, D.; Elce, J. S.; Jia, Z.; Davies, P. L. A  $\text{Ca}^{2+}$  Switch Aligns the Active Site of Calpain. *Cell* **2002**, *108*, 649–660.

(26) Moldoveanu, T.; Hosfield, C. M.; Lim, D.; Jia, Z.; Davies, P. L. Calpain Silencing by a Reversible Intrinsic Mechanism. *Nat. Struct. Biol.* **2003**, *10*, 371–378.

(27) Arad, D.; Langridge, R.; Kollman, P. A. A Simulation of the Sulfur Attack in the Catalytic Pathway of Papain Using Molecular Mechanics and Semiempirical Quantum Mechanics. *J. Am. Chem. Soc.* **1990**, *112*, 491–502.

(28) Nemukhin, A. V.; Grigorenko, B. L.; Rogov, A. V.; Topol, I. A.; Burt, S. K. Modeling of Serine Protease Prototype Reactions with the Flexible Effective Fragment Potential Quantum Mechanical/Molecular Mechanical Method. *Theor. Chem. Acc.* **2004**, *111*, 36–48.

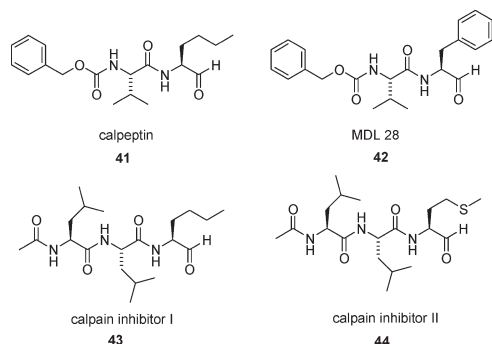
(29) Topf, M.; Varnai, P.; Richards, W. G. Ab Initio QM/MM Dynamics Simulation of the Tetrahedral Intermediate of Serine Proteases: Insights into the Active Site Hydrogen-Bonding Network. *J. Am. Chem. Soc.* **2002**, *124*, 14780–14788.

(30) The constructs consist of domains I and II which contain the active site of the enzyme.

(31) The first reports of an inhibitor bound with a calpain were the structure of domain VI of porcine CAPN2 with  $\text{Ca}^{2+}$  bound (1ALV) and with  $\text{Ca}^{2+}$  and inhibitor PD150606 (3-(4-iodophenyl)-2-mercapto-(Z)-2-propenoic acid) bound (1ALW). Lin, G.-d.; Chattopadhyay, D.; Maki, M.; Wang, K. K. W.; Carson, M.; Jin, L.; Yuen, P.-w.; Takano, E.; Hatanaka, M.; DeLucas, L. J.; Narayana, S. V. L. Crystal Structure of Calcium Bound Domain VI of Calpain at 1.9 Å Resolution and Its Role in Enzyme Assembly, Regulation, and Inhibitor Binding. *Nat. Struct. Biol.* **1997**, *No. 4*, 539–547. PD150606 was first proposed by Wang to be a nonactive site inhibitor, and correctly with his prediction the crystal structure shows it bound into a hydrophobic pocket created by three helices. Wang, K. K. W.; Nath, R.; Posner, A.; Raser, K. J.; Buroker-Kilgore, M.;

- Hajimohammadreza, I.; Probert, A. W., Jr.; Marcoux, F. W.; Ye, Q.; Takano, E.; Hatanaka, M.; Maki, M.; Caner, H.; Collins, J. L.; Fergus, A.; Lee, K. S.; Lunney, E. A.; Hays, S. J.; Yuen, P. An Alpha-Mercaptoacrylic Acid Derivative Is a Selective Nonpeptide Cell-Permeable Calpain Inhibitor and Is Neuroprotective. *Proc. Natl. Acad. Sci. U.S.A.* **1996**, *93*, 6687–6692. This is the pocket that has been shown to be the site where residue Phe610 of the endogenous calpain inhibitor calpastatin also binds. Todd, B.; Moore, D.; Deivanayagam, C. C. S.; Lin, G.; Chattopadhyay, D.; Maki, M.; Wang, K. K. W.; Narayana, S. V. L. A Structural Model for the Inhibition of Calpain by Calpastatin: Crystal Structures of the Native Domain VI of Calpain and Its Complexes with Calpastatin Peptide and a Small Molecule Inhibitor. *J. Mol. Biol.* **2003**, *328*, 131–146.
- (32) Maki, M.; Takano, E.; Mori, H.; Sato, A.; Murachi, T.; Hatanaka, M. All Four Internally Repetitive Domains of Pig Calpastatin Possess Inhibitory Activities against Calpains I and II. *FEBS Lett.* **1987**, *223*, 174–180. Kiss, R.; Kovacs, D.; Tompa, P.; Perczel, A. Local Structural Preferences of Calpastatin, the Intrinsically Unstructured Protein Inhibitor of Calpain. *Biochemistry* **2008**, *47*, 6936–6945. Jiao, W.; McDoanld, D. Q.; Coxon, J. M.; Parker, E. J. Molecular Modelling Studies on Conformations of CP1B: the 20-mer Peptide Resembling Calpastatin Inhibitory Domain Region. *Biochemistry* **2010**, *49*, 5533–5539.
- (33) Takano, E.; Maki, M. Structure of Calpastatin and Its Inhibitory Control of Calpain. In *CALPAIN: Pharmacology and Toxicology of Calcium-Dependent Protease*; Wang, K. K. W., Yuen, P.-w., Eds.; Taylor & Francis: Philadelphia, PA, 1999; pp 25–50. Averna, M.; De Tullio, R.; Salamino, F.; Melloni, E.; Pontremoli, S. Phosphorylation of Rat Brain Calpastatins by Protein Kinase C. *FEBS Lett.* **1999**, *450*, 13–16. Melloni, E.; Averna, M.; Stifanese, R.; De Tullio, R.; Defranchi, E.; Salamino, F.; Pontremoli, S. Association of Calpastatin with Inactive Calpain. A Novel Mechanism to Control the Activation of the Protease? *J. Biol. Chem.* **2006**, *281*, 24945–24954. Emori, Y.; Kawasaki, H.; Imajoh, S.; Minami, Y.; Suzuki, K. All Four Internally Repetitive Domains of Pig Calpastatin Possess Inhibitory Activities against Calpains I and II. *FEBS Lett.* **1988**, *223*, 174–180. Todd, B.; Moore, D.; Deivanayagam, C. C. S.; Lin, G. D.; Chattopadhyay, D.; Maki, M.; Wang, K. K. W.; Narayana, S. V. L. All Four Repeating Domains of the Endogenous Inhibitor for Calcium-Dependent Protease Independently Retain Inhibitory Activity. Expression of the cDNA Fragments in *Escherichia coli*. *J. Biol. Chem.* **2003**, No. 263, 2364–2370. Ma, H.; Yang, H. Q.; Takano, E.; Hatanaka, M.; Maki, M. A Structural Model for the Inhibition of Calpain by Calpastatin: Crystal Structures of the Native Domain VI of Calpain and Its Complexes with Calpastatin Peptide and a Small Molecule Inhibitor. *J. Mol. Biol.* **1994**, *328*, 131–146. Hanna, R. A.; Garcia-Diaz, B. E.; Davies, P. L. Amino-Terminal Conserved Region in Proteinase Inhibitor Domain of Calpastatin Potentiates Its Calpain Inhibitory Activity by Interacting with Calmodulin-like Domain of the Proteinase. *J. Biol. Chem.* **2007**, *269*, 24430–24436. Hanna, R. A.; Garcia-Diaz, B. E.; Davies, P. L. Calpastatin Simultaneously Binds Four Calpains with Different Kinetic Constants. *FEBS Lett.* **2007**, *581*, 2894–2898.
- (34) Donker, I. O. A Survey of Calpain Inhibitors. *Curr. Med. Chem.* **2000**, *7*, 1171–1188.
- (35) These inhibitors are limited as biomedical tools to elucidate calpain cell function because they are nonselective for calpain and exhibit poor membrane permeability, characteristics that render them poor drug candidates.
- (36) Moldoveanu, T.; Campbell, R. L.; Cuerrier, D.; Davies, P. L. Crystal Structures of Calpain-E64 and -Leupeptin Inhibitor Complexes Reveal Mobile Loops Gating the Active Site. *J. Mol. Biol.* **2004**, *343*, 1313.
- (37) Cuerrier, D.; Moldoveanu, T.; Inoue, J.; Davies, P. L.; Campbell, R. L. Calpain Inhibition by  $\alpha$ -Ketoamide and Cyclic Hemiacetal Inhibitors Revealed by X-ray Crystallography. *Biochemistry* **2006**, *45*, 7446–7452.
- (38) Qian, J.; Cuerrier, D.; Davies, P. L.; Li, Z.; Powers, J. C.; Campbell, R. L. Cocrystal Structures of Primed Side-Extending  $\alpha$ -Ketoamide Inhibitors Reveal Novel Calpain-Inhibitor Aromatic Interactions. *J. Med. Chem.* **2008**, *51*, 5264–5270.
- (39) The cocrystallized X-ray structures of the CAPN1 construct in complex with bound inhibitors confirm the earlier hypothesis of the importance of a  $\beta$ -strand conformation and that three H-bonds to Gly208 and Gly271 are essential for tight ligand binding.
- (40) Inoue, J.; Nakamura, M.; Cui, Y.; Sakai, Y.; Sakai, O.; Hill, J. R.; Wang, K. K. W.; Yuen, P. Structure–Activity Relationship and Drug Profile of *N*-(4-Fluorophenylsulfonyl)-L-valyl-L-leucinal (SJA6017) as a Potent Calpain Inhibitor. *J. Med. Chem.* **2003**, *46*, 868–871 and Supporting Information. Payne, R. J.; Brown, K. M.; Coxon, J. M.; Morton, J. D.; Lee, H. Y.-Y.; Abell, A. D. Peptidic Aldehydes Based on  $\alpha$ - and  $\beta$ -Amino Acids: Synthesis, Inhibition of m-Calpain and Anti-Cataract Properties. *Aust. J. Chem.* **2004**, *57*, 877–884.
- (41) At the beginning of this project the CAPN1 construct (1KXR) was the only X-ray crystal structure of calpain in the active conformation. Papain was also examined in detail because of the similarity of the active site with that in calpain. There are many X-ray crystal structures of papain in the PDB with and without cysteine protease inhibitors bound in the active site. Many of these inhibitors have been shown to also inhibit both CAPN1 and CAPN2.
- (42) The PDB coordinates of 1KXR are imported into Maestro, Schrodinger's graphical interface. *Maestro*, version 7.5; Schrodinger, LLC: New York, NY, 2005. The water molecules are deleted along with the second molecule of the dimer (chain B) to leave the monomer (chain A). Hydrogens are added to this chain and the active site Ser115 is mutated in silico to Cys115 to produce a structure that resembles the active site of the native enzyme. The Cys115 is deprotonated and His272 protonated in silico to simulate this mechanistic change that is considered to occur upon ligand binding with the enzyme. After minimization this structure was used for docking experiments and is referred to as the “model”. The “model” had to be modified to work with the InducedFit docking protocol because Prime, part of the InducedFit protocol, would not allow the deprotonated Cys115 in the docking procedure. Therefore, Cys115 was left protonated for InducedFit docking and is referred to as the “InducedFit model”.
- (43) Most inhibitors that bind in the active site of papain bind to the nonprime side, and it is therefore reasonable to assume that these inhibitors and their analogues will bind calpain in the nonprime side. This becomes important in setting up the docking grid, a set of coordinates that isolate and map the site on the enzyme to where ligands are to be docked.
- (44) When a conformation not in a  $\beta$ -strand was used as a starting structure, it was found that the enzyme model is not always sufficiently flexible to allow for the conformational space of the inhibitor to be explored appropriately.
- (45) Fairlie, D. P.; Tyndall, J. D. A.; Reid, R. C.; Wong, A. K.; Abbenante, G.; Scanlon, M. J.; March, D. R.; Bergman, D. A.; Chai, C. L. L.; Burkett, B. A. Conformational Selection of Inhibitors and Substrates by Proteolytic Enzymes: Implications for Drug Design and Polypeptide Processing. *J. Med. Chem.* **2000**, *43*, 1271–1281.
- (46) Reid, R. C.; Pattenden, L. K.; Tyndall, J. D. A.; Martin, J. L.; Walsh, T.; Fairlie, D. P. Countering Cooperative Effects in Protease Inhibitors Using Constrained  $\beta$ -Strand-Mimicking Templates in Focused Combinatorial Libraries. *J. Med. Chem.* **2004**, *47*, 1641–1651.
- (47) These residues had earlier been reported to be involved following studies of structures of other cysteine proteases such as papain cocrystallized with the inhibitor E-64. Yamamoto, D.; Matsumoto, K.; Ohishi, H.; Ishida, T.; Inoue, M.; Kitamura, K.; Mizuno, H. Refined X-ray Structure of Papain. E-64-c Complex at 2.1-Å Resolution. *J. Biol. Chem.* **1991**, *266*, 14771–14777. The three H-bonds were formed between the ligand, and we consider these two residues essential for stabilizing the bound ligand. Known di- and tripeptide based inhibitors of calpain usually have a capping group at the N-terminus which positions itself around the S<sub>3</sub> subsite of the enzyme. This P<sub>3</sub> subsite is surrounded by the residues Cys209, Ser251, Asn253, Lys347, and Glu349, all of which have H-bond donors or acceptors; therefore, capping groups that have H-bond acceptors or donors would likely be able to form H-bonds with these residues. Such H-bond formation will increase the binding affinity of the ligand, and to improve selectivity and

permeability, N-terminal capping groups have been modified with lipophilic substituents.<sup>34</sup> Calpeptin (**44**) (Tsujinaka, T.; Kajiura, Y.; Kambayashi, J.; Sakon, M.; Higuchi, N.; Tanaka, T.; Mori, T. Synthesis of a New Cell Penetrating Calpain Inhibitor (Calpeptin). *Biochem. Biophys. Res. Commun.* **1988**, *153*, 1201–1208. ), MDL 28 (**42**) (Mehdi, S.; Angelastro, M. R.; Wiseman, J. S.; Bey, P. Inhibition of the Proteolysis of Rat Erythrocyte Membrane Proteins by a Synthetic Inhibitor of Calpain. *Biochem. Biophys. Res. Commun.* **1988**, *157*, 1117–1123. ), calpain inhibitor I (**43**), and calpain inhibitor II (**44**) all showed improved cell permeability (Sasaki, T.; Kishi, M.; Saito, M.; Tanaka, T.; Higuchi, N.; Kominami, E.; Katunuma, N.; Murachi, T. Inhibitory Effect of Di- and Tripeptidyl Aldehydes on Calpains and Cathepsins. *J. Enzyme Inhib.* **1990**, *3*, 195–201), and SAR (structure–activity relationship) data showed these compounds to be more potent than the unmodified natural inhibitors. They all, however, lack selectivity for calpain that limits their therapeutic potential. For example, **43** is more potent against cathepsin than calpain.



(48) Several structures of the calpain construct with inhibitors bound in the active site have recently been published and show subtle changes in the active site relative to 1KXR to accommodate their bound ligands.

(49) An “ugly” internal contact reflects the molecule being forced to fit into the active site. The Glide docking program keeps the enzyme rigid and not able to move to accommodate such a ligand without unfavorable internal contacts.

(50) Nikkel, J. M. The Design, Synthesis and Biological Assay of Cysteine Protease Specific Inhibitors. Ph.D. Thesis, University of Canterbury, Christchurch, New Zealand, 2007.

(51) Most of these “ugly” contacts result from the P<sub>1</sub> and P<sub>2</sub> side chains being too close to each other along with the P<sub>2</sub> side chain being proximate to the phenyl ring in the capping group.

(52) The X-ray structures of these two  $\alpha$ -ketoamides show their capping groups sitting over Gly208 similar to observations in the modeling of several of the Inoue<sup>40</sup> compounds. The CBz group of the two  $\alpha$ -ketoamides has no substituents on the aromatic ring that can act as hydrogen bond donors or acceptors.

(53) Jones, M. A.; Morton, J. D.; Coxon, J. M.; McNabb, S. B.; Lee, H. Y.-Y.; Aitken, S. G.; Mehrtens, J. M.; Robertson, L. J. G.; Neffe, A. T.; Miyamoto, M.; Bickerstaffe, R.; Gately, K.; Wood, J. M.; Abell, A. D. Synthesis, Biological Evaluation and Molecular Modeling of N-Heterocyclic Dipeptide Aldehydes as Selective Calpain Inhibitors. *Bioorg. Med. Chem.* **2008**, *16*, 6911–6923. Abell, A. D.; Coxon, J. M.; Miyamoto, S.; Jones, M. A.; Neffe, A. T.; Aitken, S. G.; Stuart, B. G.; Nikkel, J. M.; Morton, J. D.; Bickerstaffe, R.; Robertson, L. J. G.; Lee, H. Y.-Y.; Muir, M. S. Preparation of Peptide Alcohols and Aldehydes as Calpain Inhibitors. Patent NZ 547303(A), 2007.

(54) For further information, see the following. Stuart, B. G. Molecular Modelling for Enzyme-Inhibition: A Search for a New Treatment for Cataract and Antimicrobials and Herbicides. Ph.D. Thesis, University of Canterbury, Christchurch, New Zealand, 2010.

(55) However, this unusual binding pattern has some “ugly” internal contacts and the valine at the P<sub>2</sub> position is pointing out of the pocket instead of pointing into the hydrophobic S<sub>2</sub> subsite which is more typical of potent dipeptides.

(56) Glenn, P.; Pattenden, L. K.; Reid, R. C.; Tyssen, D. P.; Tyndall, J. D. A.; Birch, C. J.; Fairlie, D. P.  $\beta$ -Strand Mimicking Macrocyclic Amino Acids: Templates for Protease Inhibitors with Antiviral Activity. *J. Med. Chem.* **2002**, *45*, 371–381.

(57) Lucke, A. J.; Tyndall, J. D. A.; Fairlie, D. P. Designing Supramolecular Structures from Models of Cyclic Peptide Scaffolds with Heterocyclic Constraints. *J. Mol. Graphics Modell.* **2003**, *21*, 341–355.

(58) Abell, A. D.; Alexander, N. A.; Aitken, S. G.; Chen, H.; Coxon, J. M.; Jones, M. A.; McNabb, S. B.; Muscroft-Taylor, A. The Synthesis of Macrocyclic  $\beta$ -Strand Templates by Ring Closing Metathesis. *J. Org. Chem.* **2009**, *74* (11), 4354–4356.

(59) Jones, M. A.; Coxon, J. M.; McNabb, S. B.; Mehrtens, J. M.; Alexander, N. A.; Jones, S.; Chen, H.; Buisan, C.; Abell, A. D. Efficient Large-Scale Synthesis of CAT811, a Potent Calpain Inhibitor of Interest in the Treatment of Cataract. *Aust. J. Chem.* **2009**, *62* (7), 671–675.

(60) Some of the compounds did not dock when a turn-type conformation was used as a starting structure, but redocking from the lowest energy  $\beta$ -strand conformation proved to be advantageous. However, some would still not dock with poses that met our criteria of having the three essential H-bonds, close warhead–nucleophile distance, and low Glide and Emodel scores. Docking studies were then performed with the InducedFit protocol, which takes up more computer time but was thought to be necessary because of the larger size of the macrocycles compared with the acyclic dipeptides we had previously studied. The InducedFit protocol allows the active site to make small adjustments with respect to each docked ligand, thereby simulating what effectively happens in a real enzyme. InducedFit docking showed that compounds **A1**, **A3**, **A4**, **B1**, and **B3** could dock into the enzyme model with all the criteria met. With this evidence **A1** and **B1** were synthesized and tested in vitro and proved to inhibit CAPN2 with IC<sub>50</sub> of 3710 and 280 nM, respectively. This was sound evidence that the modeling and docking experiments were providing relevant information to guide the synthetic chemists to synthesizing appropriate compounds from the macrocyclic library.

(61) Abell, A. D.; Coxon, J. M.; Jones, M. A.; McNabb, S. B.; Neffe, A. T.; Aitken, S. G.; Stuart, B. G.; Nikkel, J. M.; Duncan, J. K.; Klanchantra, M.; Morton, J. D.; Bickerstaffe, R.; Robertson, L. J. G.; Lee, H. Y. Y.; Muir, M. S. Preparation of Macrocyclic Peptide Alcohols and Aldehydes as Calpain Inhibitors and Their Compositions. Patent US 2011021434 (A1) 2011, 2011. Aitken, S. G. Design, Synthesis and Testing of  $\beta$ -Strand Mimics as Protease Inhibitors. Ph.D. Thesis, University of Canterbury, Christchurch, New Zealand, 2006.

(62) The Boltzmann weighted percentage of  $\beta$ -strand for each macrocycle was based on the  $\psi$  and  $\phi$  angles of the P<sub>2</sub> amino acid. Ramachandran plots of  $\psi$ ,  $\phi$  angles for  $\beta$ -strand or  $\beta$ -sheet regions of protein X-ray crystal structures show that typical  $\psi$  angles are between 90° and 160° and that  $\phi$  angles are between –90° and –160°. Griffiths-Jones, S. R.; Sharman, G. J.; Maynard, A. J.; Searle, M. S. Modulation of Intrinsic f<sub>c</sub> Propensities of Amino Acids by Neighbouring Residues in the Coil Regions of Protein Structures: NMR Analysis and Dissection of a  $\beta$ -Hairpin Peptide. *J. Mol. Biol.* **1998**, *284*, 1597–1609. These parameters were consequently used to determine the Boltzmann weighted percentage of  $\beta$ -strand for each macrocycle.

(63) **A1**, **A2**, **A18**, **H1**, **I9**, **P7**, and **P8** are the only compounds in the library that have a >90% preference for a  $\beta$ -strand conformation and were docked using in each case the lowest energy conformer in a  $\beta$ -strand and the InducedFit protocol.

(64) Carragher, N. O. Calpain Inhibition: A Therapeutic Strategy Targeting Multiple Disease States. *Curr. Pharm. Des.* **2006**, *12*, 615–638.

(65) Cysteine proteases have been problematic for drug design, as many of their known inhibitors contain an electrophilic “warhead” that binds covalently in a reversible or irreversible manner making the inhibitor particularly reactive such that they can bind nonspecifically to proteins, receptors, and biomolecules in vivo. This can give rise to problems with toxicity associated with drug metabolism and pharmacokinetics. Lindvall, M. K. Molecular Modeling in Cysteine Protease Inhibitor Design. *Curr. Pharm. Des.* **2002**, *8*, 1673–1681. Schneek, J. L.;



Villa, J. P.; McDevitt, P.; McQueney, M. S.; Thrall, S. H.; Meek, T. D. Chemical Mechanism of a Cysteine Protease, Cathepsin C, As Revealed by Integration of both Steady-State and Pre-Steady-State Solvent Kinetic Isotope Effects. *Biochemistry* **2008**, *47*, 8697–8710. There is therefore interest in developing selective inhibitors that can address such problems.

(66) Abell, A. D.; Jones, M. A.; Coxon, J. M.; Morton, J. D.; Aitken, S. G.; McNabb, S. B.; Lee, H. Y.-Y.; Mehrtens, J. M.; Alexander, N. A.; Stuart, B. G.; Neffe, A. T.; Roy Bickerstaffe, R. Molecular Modeling, Synthesis, and Biological Evaluation of Macrocyclic Calpain Inhibitors. *Angew. Chem., Int. Ed.* **2009**, *48*, 1455–1458 and supplementary material.

(67) Lindvall, M. K. Molecular Modeling in Cysteine Protease Inhibitor Design. *Curr. Pharm. Des.* **2002**, *8*, 1673–1681. Schneck, J. L.; Villa, J. P.; McDevitt, P.; McQueney, M. S.; Thrall, S. H.; Meek, T. D. Chemical Mechanism of a Cysteine Protease, Cathepsin C, As Revealed by Integration of Both Steady-State and Pre-Steady-State Solvent Kinetic Isotope Effects. *Biochemistry* **2008**, *47*, 8697–8710.

(68) Cuerrier, D.; Moldoveanu, T.; Inoue, J.; Davies, P. L.; Campbell, R. L. Calpain Inhibition by  $\alpha$ -Ketoamide and Cyclic Hemiacetal Inhibitors Revealed by X-ray Crystallography. *Biochemistry* **2006**, *45*, 7446–7452.

(69) Despite the model being based on a CAPN1 construct (1KXR) and our ultimate goal being the design of inhibitors of the cataract causing CAPN2, the model has been a success. An CAPN2 model would have been a more appropriate model, but this was not possible because there is no X-ray crystal structure of an active CAPN2. However, CAPN1 and CAPN2 are very similar in their active site structures and most inhibitors of one form inhibit the other, and this warranted the use of the CAPN1 construct as a model to perform docking experiments.

(70) *MacroModel*, version 9.1; Schrödinger, LLC: New York, NY, 2005.

(71) *Glide*, version 4.0; Schrödinger, LLC: New York, NY, 2005.

(72) *InducedFit Docking Protocol*, *Schrödinger Suite 2006*. *Glide*, version 4.0; Schrödinger, LLC: New York, NY, 2005. *Prime*, version 1.5; Schrödinger, LLC: New York, NY, 2005

(73) Thompson, V. F.; Saldana, S.; Cong, J.; Goll, D. E. A BODIPY Fluorescent Microplate Assay for Measuring Activity of Calpains and Other Proteases. *Anal. Biochem.* **2000**, *279*, 170–178.